

IFUSP/P 636  
B.L.F. - USF

UNIVERSIDADE DE SÃO PAULO

# PUBLICAÇÕES

INSTITUTO DE FÍSICA  
CAIXA POSTAL 20516  
01498 - SÃO PAULO - SP  
BRASIL

IFUSP/P-636

BIFURCATIONS OF PERIODIC SOLUTIONS OF  
NON-INTEGRABLE HAMILTONIANS WITH TWO DEGREES  
OF FREEDOM: NUMERICAL AND ANALYTICAL RESULTS

27 JUL 1987



M.A.M. de Aguiar, C.P. Malta  
Instituto de Física, Universidade de São Paulo

M. Baranger  
Dept. of Physics, Massachusetts Institute of  
Technology, Cambridge, MA 02139

and

K.T.R. Davies  
Physics Division, Oak Ridge National Laboratory,  
Oak Ridge, TN 37831 and  
Dept. of Physics, Massachusetts Institute of  
Technology, Cambridge, MA 02139

Abril/1987

# BIFURCATIONS OF PERIODIC SOLUTIONS OF NON-INTEGRABLE HAMILTONIANS

## WITH TWO DEGREES OF FREEDOM: NUMERICAL AND ANALYTICAL RESULTS

M.A.M. de Aguiar, C.P. Malta

Instituto de Física, Universidade de São Paulo  
C.P. 20516, 01498 São Paulo, SP, Brazil

M. Baranger

Dept. of Physics, Massachusetts Institute of  
Technology, Cambridge, MA 02139

and

K.T.R. Davies

Physics Division, Oak Ridge National Laboratory,  
Oak Ridge, TN 37831

and

Dept. of Physics, Massachusetts Institute of  
Technology, Cambridge, MA 02139

### ABSTRACT

We present an analytical study of the bifurcations of periodic solutions observed numerically in a two-dimensional non-integrable Hamiltonian system with two-degrees of freedom.

### 1. INTRODUCTION

In this work we present the results of an extensive numerical investigation of the periodic solutions of a two-dimensional non-integrable Hamiltonian system with two degrees of freedom. We also present an analytic study of the types of bifurcations that a periodic trajectory may undergo and which were "experimentally" observed.

Our desire to understand the problem of quantization was our main motivation. The problem of quantization arises naturally when one deals with many-body problems, as there are easy to obtain approximate solutions of the many-body Schrödinger equation which consist of wave-packets evolving in time along classical-like trajectories. All the time dependent mean field approximations<sup>1</sup> are of this type, the time-dependent Hartree-Fock being the best known case.

As is well known<sup>2</sup>, the periodic trajectories form one-parameter families. The energy  $E$  or the period  $\tau$  are two convenient labelling parameters for a particular trajectory within its family. Most of our data are presented in the form of  $E$ - $\tau$  plots, each periodic family being represented by a continuous line in the  $E$ - $\tau$  plane. This set of lines is characteristic of the Hamiltonian  $H$ , and its branchings determine the topology of the  $E$ - $\tau$  plot. We shall see that the symmetries of  $H$  have an important effect on what kinds of

branchings occur.

A very useful way of characterizing a periodic trajectory is by its monodromy<sup>3</sup> matrix  $M$  (also called Liapunov matrix). For two dimensions this is a  $4 \times 4$  matrix describing the dependence on the initial conditions of the trajectory after one period. It is a symplectic matrix<sup>3</sup>, always with two unit eigenvalues. The two other eigenvalues can be either complex conjugates (of the form  $e^{i\alpha}$ ,  $e^{-i\alpha}$ ) or real (of the form  $e^{\beta}$ ,  $e^{-\beta}$ ), corresponding to stable and unstable trajectories respectively. We shall show in section 2 how these well-known properties of the monodromy matrix are modified by the discretization of the time-axis which is necessary to perform numerical calculations.

In this work we shall consider the following Hamiltonian

$$H = \frac{p_x^2}{2} + \frac{p_y^2}{2} + \frac{x^2}{2} + \frac{3y^2}{2} - x^2y + \frac{x^4}{12} \quad (1.1)$$

Our code name for this particular system is MARTA. The detailed numerical investigation presented here was made possible by the development of a new computational method<sup>4</sup> which is especially adapted to the search for periodic trajectories and which works equally well for stable and unstable solutions. This is important since periodic families exhibit more than one region of stability and this property allows us to follow completely

the families generated by the normal modes at the minimum of the potential. To date, four different two-dimensional potential systems have been investigated thoroughly by this method<sup>5</sup>. Three of these, including the present one (1.1), are symmetric under the reflection  $x \rightarrow -x$ . Since all four Hamiltonians also possess time-reversal symmetry, we have in these three systems a doubly symmetric situation, which turns out to have important consequences for the kinds of branchings to be expected.

We have calculated roughly 2,000 periodic trajectories comprising roughly 50 families for the MARTA Hamiltonian. Some of these results are presented in section 3. Section 4 contains a complete summary of the possible types of bifurcations in the families of periodic trajectories, for Hamiltonians which may have 0, 1, or 2 symmetries, as revealed by our numerical studies and those of references 5 and 6. An analytical study of this subject was carried out by Meyer<sup>7</sup>, but he confined himself to the "generic" case of Hamiltonians without symmetry. In section 5 we extend the work of Meyer to include Hamiltonians with time-reversal symmetry and space-reflexion symmetry, and we find that these two symmetries are responsible for the additional types of bifurcations which show up in the numerical work.

## 2. THE DISCRETIZED MONODROMY MATRIX

We shall study the discretized monodromy matrix for a two-dimensional Hamiltonian of the form

$$H(x, p_x, y, p_y) = \frac{p_x^2}{2} + \frac{p_y^2}{2} + V(x, y) . \quad (2.1)$$

Extension to higher dimensionality is immediate.

Extension to other types of Hamiltonians is possible.

Newton's equations of motion for (2.1) are

$$\begin{aligned} \ddot{x} &= - \frac{\partial V(x, y)}{\partial x} = -v_x(x, y) , \\ \ddot{y} &= - \frac{\partial V(x, y)}{\partial y} = -v_y(x, y) , \end{aligned} \quad (2.2)$$

a dot meaning derivative with respect to time.

The monodromy (or Liapunov) matrix<sup>3</sup> gives the change in the solution of (2.2) after one period, in terms of the change in the initial conditions. It is therefore quite suitable for an iterative numerical procedure that produces a periodic solution of (2.2) starting from a periodic approximation to it. Such a procedure is described in reference 4. Here we shall confine ourselves to studying the monodromy matrix of a periodic trajectory which is already an exact solution.

Since we are doing numerical work, however, we must

discretize eqs. (2.2). Let us specify the trajectory by  $N$  points equally spaced in time  $(x_n, y_n)$ ,  $n = 0, 1, 2, \dots, N-1$ . Let  $\epsilon$  be the time step and  $\tau = N\epsilon$  the period. Periodicity is expressed by

$$(x_0, y_0) = (x_N, y_N) , \quad (x_1, y_1) = (x_{N+1}, y_{N+1}) . \quad (2.3)$$

We use the simplest discretization of (2.2), namely

$$\begin{aligned} x_{n+1} - 2x_n + x_{n-1} + \epsilon^2 v_x(x_n, y_n) &= 0 , \\ y_{n+1} - 2y_n + y_{n-1} + \epsilon^2 v_y(x_n, y_n) &= 0 . \end{aligned} \quad (2.4)$$

The application of our numerical method yields an exact periodic solution  $(x_n, y_n)$  of eqs. (2.4) for a given  $\epsilon$ , and in the following we shall assume that this has been done.

Suppose now that we want to look for another solution  $(x_n + \delta x_n, y_n + \delta y_n)$  of (2.4) in the vicinity of the first. This solution will generally be non-periodic. To obtain it, we linearize (2.4) in the vicinity of the original solution, assuming  $\delta x_n$  and  $\delta y_n$  small:

$$\begin{aligned} \delta x_{n+1} - 2\delta x_n + \delta x_{n-1} + \epsilon^2 v_{xx}(x_n, y_n) \delta x_n + \epsilon^2 v_{xy}(x_n, y_n) \delta y_n &= 0 \\ \delta y_{n+1} - 2\delta y_n + \delta y_{n-1} + \epsilon^2 v_{yx}(x_n, y_n) \delta x_n + \epsilon^2 v_{yy}(x_n, y_n) \delta y_n &= 0 . \end{aligned} \quad (2.5)$$

.7.

Defining the vector

$$z_n = \begin{pmatrix} \delta x_n \\ \delta y_n \\ \delta x_{n-1} \\ \delta y_{n-1} \end{pmatrix}, \quad (2.6)$$

we can cast eqs. (2.5) in the form

$$z_{n+1} = U_n z_n \quad (2.7)$$

where  $U_n$  is a  $4 \times 4$  matrix which, written in terms of  $2 \times 2$  blocks, looks as follows

$$U_n = \begin{pmatrix} P_n & -\mathbf{1} \\ \mathbf{1} & 0 \end{pmatrix}, \quad (2.8)$$

with

$$P_n = \begin{pmatrix} 2 - \epsilon^2 v_{xx}(x_n, y_n) & -\epsilon^2 v_{xy}(x_n, y_n) \\ -\epsilon^2 v_{yx}(x_n, y_n) & 2 - \epsilon^2 v_{yy}(x_n, y_n) \end{pmatrix}. \quad (2.9)$$

Using (2.7) recurrently we get

.8.

$$z_{N+1} = M_1 z_1 \quad (2.10)$$

where  $M_1$  is the discretized monodromy matrix, given by

$$M_1 = U_N U_{N-1} \dots U_2 U_1 \quad (2.11)$$

The inverse of  $U_n$  is easily seen to be

$$U_n^{-1} = \begin{pmatrix} 0 & \mathbf{1} \\ -\mathbf{1} & P_n \end{pmatrix} \quad (2.12)$$

and it can be immediately verified that  $U_n$  has the symplectic property

$$U_n^{-1} = \Lambda U_n^T \Lambda^{-1}, \quad (2.13)$$

where  $\Lambda$  is the  $4 \times 4$  matrix

$$\Lambda = \begin{pmatrix} 0 & \mathbf{1} \\ -\mathbf{1} & 0 \end{pmatrix} \quad (2.14)$$

and the superscript  $T$  denotes transposition. The matrix  $\Lambda$  satisfies the relations

$$\begin{aligned} \Lambda^2 &= -\mathbf{1} \\ \Lambda^{-1} &= \Lambda^T = -\Lambda \end{aligned} \quad (2.15)$$

By inverting both sides of eq. (2.11) and using (2.13), we find that the monodromy matrix possesses the symplectic property as well, i.e.

$$M_1^{-1} = \Lambda M_1^T \Lambda^{-1} \quad (2.16)$$

This relation says that  $M_1^{-1}$  and  $M_1^T$  have the same eigenvalues. Since  $M_1$  and  $M_1^T$  have the same eigenvalues, it follows that  $M_1^{-1}$  and  $M_1$  have the same eigenvalues. Therefore the eigenvalues of  $M_1$  occur in pairs of inverses. This is a well-known property of the continuum monodromy matrix<sup>3</sup>. The above argument shows that it is also an exact property of the discretized one.

We recall that the original trajectory  $(x_n, y_n)$  was periodic, i.e. it satisfies eqs. (2.3). If we want the neighbour trajectory  $(x_n + \delta x_n, y_n + \delta y_n)$  to be periodic also, we must have  $Z_{n+1} = Z_1$ . According to (2.10), this means that  $Z_1$  must be an eigenvector of  $M_1$  for eigenvalue 1. But we actually know another, close-by, periodic solution of eqs. (2.4), namely that solution in which every  $(x_n, y_n)$  has been replaced by  $(x_{n+1}, y_{n+1})$  or, in other words, the identical trajectory with the points relabelled. The  $Z_1$  corresponding to this "neighbour" is

$$Z_1 = \begin{pmatrix} x_2 - x_1 \\ y_2 - y_1 \\ x_1 - x_0 \\ y_1 - y_0 \end{pmatrix} \quad (2.17)$$

This  $Z_1$  is not infinitesimal and, consequently, the present argument is only approximate. Within this approximation, however, the above  $Z_1$  must be an eigenvector of  $M_1$  for eigenvalue unity. Our numerical work shows that, for small values of  $\epsilon$  (for instance  $N=100$  in the case of a relatively simple trajectory, more for complicated ones), the approximation is actually excellent and the monodromy matrix has an eigenvalue which is very close to 1. Therefore, by the theorem of the previous paragraph, it also has a second eigenvalue very close to 1, which is the exact inverse of the first one. We find also that, for both eigenvalues, the eigenvector is very close to (2.17).

The two other eigenvalues of  $M_1$  must have unit product. And the complex conjugate of every eigenvalue must also be an eigenvalue, because  $M_1$  is real. This leads to two possible cases. In one case, which we shall call case S, the eigenvalues are  $(e^{+i\alpha}, e^{-i\alpha})$ , i.e. they have unit modulus and are complex conjugates. In this case, the trace of the monodromy matrix is

$$\text{Tr } M_1 = 2(1 + \cos \alpha) \quad (2.18)$$

and therefore

$$0 < \text{Tr } M_1 < 4 \quad (\text{case S}) \quad (2.19)$$

In the other case, which we shall call case U, the eigenvalues are real and can be either  $(e^\beta, e^{-\beta})$  or  $(-e^\beta, -e^{-\beta})$ . The trace of  $M_1$  is then

$$\text{Tr } M_1 = 2(1 \pm \cosh \beta) \quad (2.20)$$

which leads to

$$\text{Tr } M_1 > 4 \quad \text{or} \quad \text{Tr } M_1 < 0 \quad (\text{case U}) \quad (2.21)$$

It is well-known<sup>3</sup> that these eigenvalues determine the stability of periodic trajectory. According to the stability theorem due to Lyapunov<sup>3</sup>, most of the trajectories belonging to case S are stable, except for a set of measure zero corresponding to some values of  $\alpha$  which are rational multiples of  $2\pi$ , and all the trajectories belonging to case U are unstable. Therefore, to simplify matters, we shall refer to those regions in which inequality (2.19) is satisfied as stable regions, and to those regions in which inequality (2.21) is satisfied as unstable regions. It is very nice that one can determine the stability or instability, simply by looking at the trace of the monodromy matrix, without having to solve any eigenvalue equation. This

is true only in two dimensions, not in higher dimensionalities.

When  $M_1$  has an eigenvector  $Z_1$  with eigenvalue  $e^{\pm i\alpha}$ , where  $\alpha = 2\pi\ell/k$ ,  $\ell$  and  $k$  being non-commensurate integers with  $\ell < k$ , it is evident that by propagating  $Z_1$  around the trajectory  $k$  times one returns with the initial value, i.e. one manufactures a periodic trajectory whose period is  $k$  times the period of the original one. Thus, such points are bifurcation points for period  $k$ -upling. We actually find the period-multiplied trajectories by following this procedure. These bifurcation points are everywhere dense on the interval (2.19), but we limit ourselves to the simplest values of  $k$ ,  $k = 1$  to 6, for obvious reasons. In particular we have a period-tripling when  $\text{Tr } M_1 = 1$  and a period-quadrupling when  $\text{Tr } M_1 = 2$ . The period-doubling case,  $k = 2$ ,  $\text{Tr } M_1 = 0$ , is special because it corresponds to the edge of the interval of stability. At the other end of this interval, we have  $\text{Tr } M_1 = 4$ , all four eigenvalues equal to 1. This is where one should find the isochronous branchings ("no change of period"), when two distinct families, each with its own pair of eigenvalues equal to 1, coalesce into one. We shall give more discussion of the various types of branchings in sections 4 and 5.

### 3. NUMERICAL RESULTS

We present here approximately 50 families of periodic trajectories of the MARTA Hamiltonian (1.1). Its potential  $V(x,y)$  is

$$V(x,y) = \frac{x^2}{2} + \frac{x^4}{12} + \frac{3y^2}{2} - x^2y \quad (3.1)$$

Its equipotential lines are shown in fig. 1. It was the first potential to be investigated by our method. We chose it because it resembled the Henon-Heiles<sup>8</sup> potential, and because it had less symmetry, which made it easier for us at the time to find the low-energy families. The minimum is at the origin with  $V=0$ . There are two saddle points at  $(x,y) = (\pm\sqrt{3}, 1)$ ,  $V = \frac{3}{4}$ . The families issuing from the small oscillations about the origin in the horizontal ( $x$ ) and vertical ( $y$ ) directions are called H and V, respectively. The V family has constant period ( $\tau = 2\pi/\sqrt{3}$ ) since the potential is harmonic for  $x=0$ . This is not true of  $V(x,0)$ . The families issuing from the transversal oscillations (in directions of slope  $\mp 2/\sqrt{3}$ ) about the saddle points  $(\pm\sqrt{3}, 1)$  are labelled  $S_{\pm}$ . When a family F undergoes a period  $n$ -upling bifurcation, the new families branching off are labelled  $Fna$ ,  $Fnb$  and so on. When  $Fna$  undergoes a period  $m$ -upling bifurcation, the new families are labelled  $Fnama$ ,  $Fnamb$ , and so on. In the case of isochronous

( $n=1$ ) bifurcation the  $n$  is omitted.

The  $E-\tau$  plots for the H family and its branchings and for the V family and its branchings are shown in figures 2 and 3 respectively. The  $E-\tau$  plot for the  $S_{\pm}$  families is shown in figure 4. The symbol  $\rho$  indicates that the family is a rotation; otherwise it is a libration<sup>9</sup>. We use heavy lines or the symbol S to indicate the regions of stability of a family and thin lines or the symbol U to indicate the regions of instability. The points corresponding to the limiting values of  $\text{tr} M$ , 4 and zero (Z), are also marked in the  $E-\tau$  plots. The symbol  $Z^2$  is used when  $\text{Tr} M=0$  and  $\frac{d \text{Tr} M}{dE} = 0$ ,  $\bar{4}$  is used when  $\text{Tr} M=4$  and  $\frac{dE}{d\tau} = 0$  and  $4^2$  when  $\text{tr} M=4$  and  $\frac{d \text{Tr} M}{dE} = 0$  (see figure 5).

The saddle point families  $S_{\pm}$  are always unstable and, therefore, do not exhibit any period  $n$ -upling bifurcation (some values of  $\text{Tr} M$  are indicated in figure 4). As for the H and V families, they exhibit more than one interval of stability: H has 2 intervals and V has several, which get smaller and smaller as energy increases.

In figure 2 it is seen that the families V2a, V2b and V2aa form a loop showing that V2a and V2b are in fact the same family. This is shown in detail in figure 6 where we have intentionally enlarged the width of the cycles to show the topology of the curve. The rotation V2aa acts like a bridge connecting the two stable regions of the libration.



The first period tripling of  $V$  has a complicated topology shown separately in figure 7.

We found that the horizontal and vertical families are connected by a rotation,  $V_a = H_b$ , which bifurcates isochronously at both ends, as shown in figure 8.

For an integrable system, all families of periodic trajectories branch off one of the two basic families, which are obtained by setting one of the two actions equal to zero. This is not true in a non-integrable system. In fact, in our case, we found families which are isolated on the  $E-\tau$  plot and do not connect with the horizontal or the vertical families.

The  $E-\tau$  plots for these isolated families have the shape of an eight as shown in figure 9 (intentionally enlarged). These families have regions of stability starting (or ending) at the maximum and minimum of the energy. A group of these families is shown in figure 10. Notice that most of them have a rotation connecting, by isochronons branching, the two regions of stability at the maximum and minimum of the curve. In figure 11 we display a sequence of trajectories (projected on the  $x-y$  plane) for such a rotation, namely family  $F_a$ , which branches off the isolated family  $F$ . We shall see in section 4 that the existence of this isochronous bridge requires at least one symmetry for the original trajectory, either time-reversal or  $x$ -reversal symmetry. In other words, the trajectory must be either a libration or an  $x$ -symmetric

rotation<sup>9</sup>.

Figure 12 shows an isolated family of asymmetric rotations which does not have such an isochronous connection.

Figure 13 is an  $x-y$  plot of some member trajectories of the  $H$  family at low energy superimposed over the equipotential lines of  $V(x,y)$ . Figure 14 is the same thing for some members of the family  $S_+$ . In figure 15 we show the  $x-y$  plot of the trajectories generated at several bifurcation points of the  $H$  family. Figure 16 shows a detail of the  $E \times \tau$  plot of the period tripled families  $Ha3a$ ,  $Ha3b$ .

Our numerical study has shown that the bifurcations of a periodic family can be classified in a few definite categories. These categories remain the same for all the Hamiltonian systems which have been investigated<sup>5</sup> (detailed results for one of them are given in reference 6). The findings are summarized below in the next section.

#### 4. BIFURCATIONS OF PERIODIC TRAJECTORIES: SUMMARY OF NUMERICAL RESULTS

It is important for this discussion to realize that the periodic trajectories we are considering may have one or both of two different symmetries. One is time-reversal symmetry or  $t$ -symmetry: a libration is  $t$ -symmetric, a rotation is not<sup>9</sup>. For a time-reversal-invariant Hamiltonian, which is the case

here, every periodic solution which is a rotation has a companion solution which is the time-reversed of the first, and which consists of the same x-y trajectory described in the opposite direction. For present purposes, we consider these two rotations as two different periodic trajectories belonging to two different families. A libration, on the other hand, is its own time reversed and constitutes a single entity from the point of view of t-symmetry.

The other possible symmetry is x-symmetry, which is possible for the present potential because  $V(-x,y) = V(x,y)$ . A trajectory which is x-symmetric will simply be called "symmetric" from now on, since we have appropriate words already, namely "libration" and "rotation", to describe t-symmetry. Thus we have four kinds of trajectories: symmetric librations (2 symmetries), asymmetric librations and symmetric rotations (1 symmetry), asymmetric rotations (0 symmetry). Again, every asymmetric trajectory has a companion asymmetric trajectory which is the x-reflection and/or the t-reflexion of the first. Thus, an asymmetric rotation always belongs to a quartet.

An analytic study of the bifurcations of periodic trajectories was made by Meyer<sup>7</sup> in the case of Hamiltonian systems without symmetries ("generic case"). Therefore we had to extend his work to include the two symmetries mentioned above. This extension is presented in section 5 of this paper. The results agree exactly with our empirical findings. It is

interesting that x-symmetry and t-symmetry play exactly the same role in these results, as one might expect from the interchangeability of coordinates and momenta in the canonical formalism; the only thing that matters is the total number of symmetries,  $N_S$ , which can be 2, 1, or 0. Bifurcations with preservation of symmetry correspond to the generic case<sup>7</sup>. Other types of bifurcation result from loss of one symmetry,  $\Delta N_S = -1$ . The case  $\Delta N_S = -2$  is forbidden because the Poincaré index<sup>10</sup> must be conserved and, as mentioned before, in this case we would have 4 trajectories with the same stability.

In the following, we describe the topology of the  $E \times \tau$  plot in the vicinity of a bifurcation. We also describe the fixed points of the so called Poincaré map<sup>2</sup> which is used in the above mentioned analytic study. For a fixed energy, the Poincaré map  $P$  is the map of a plane  $x = \text{const}$  (or  $y = \text{const}$ ) on itself defined by the consecutive intersections, with  $p_x > 0$  ( $p_y > 0$ ), of this plane and the phase space trajectories lying in the vicinity of the periodic trajectory undergoing bifurcation. The point where this periodic trajectory intersects the plane is a fixed point of the map  $P$ . A period  $n$ -upling trajectory corresponds to  $n$  fixed points of the map  $P^n$ . The Poincaré map is an area preserving map and the jacobian of its linear approximation is the monodromy matrix. A stable (unstable) periodic trajectory corresponds to an elliptic (hyperbolic)<sup>2</sup> fixed point.

We call  $E_b$  the energy of the bifurcation point and  $\tau_b$  the corresponding period. We set  $E = E_b + \epsilon$  and  $\epsilon$  is the parameter which is varied as we cross the bifurcation point. We shall consider only the case of the bifurcated trajectories appearing for  $\epsilon > 0$  as the situation for  $\epsilon < 0$  is completely analogous. A full (dashed) line is here used to indicate a stable (unstable) family. Thick lines (full or dashed) indicate that there are two degenerate families branching off the bifurcation point.

In table 1 we present the  $E \times \tau$  plot in the vicinity of an isochronous bifurcation ( $\text{Tr} M = 4$ ) together with the fixed points of  $P$ . We indicate the number of symmetries  $N_S$  of the bifurcating trajectory and the variation  $\Delta N_S$ . In tables 2 to 5 we present the  $E \times \tau$  plot and the fixed points of  $P^n$  for period  $n$ -upling ( $n \geq 2$ ) bifurcations.

The period  $n$ -upling bifurcations of the  $V$  family,  $n$  odd  $> 3$ , are different therefore we display them separately in table 6. The period  $2n$ -upling bifurcations of the  $V$  family are generic, the bifurcated trajectories being symmetric librations (the  $V$ -family does not have  $z^2$  or  $4^2$  branching points).

Remarks - 1) We did not find any  $4^2$  branching for the MARTA potential but it was found in some of the other potentials<sup>5</sup> therefore, for completeness, we present this bifurcation here.  
2) The numerical results do not go beyond period 6-upling.

## 5. BIFURCATIONS OF SYMMETRIC PERIODIC TRAJECTORIES: ANALYTIC STUDY

As already mentioned, we follow the method of Meyer<sup>7</sup> extending it to take symmetries into account.

The Poincaré map introduced in section 4 is generated by a reduced Hamiltonian defined as follows. Let  $\Gamma_1$  be the projection of a periodic trajectory on the  $(x, p_x)$  plane (figure 17a). We define the action angle variables  $I_1, \phi_1$  so that

$$I_1 = 2\pi \oint_{\Gamma_1} p_x dx \quad (5.1)$$

and  $\phi_1$  is such that  $\dot{\phi}_1 = 2\pi/\tau$  ( $\tau$  is the period of the trajectory). Using energy conservation

$$H(x, p_x, y, p_y) = H(I_1, \phi_1, p_y, y) = E \quad (5.2)$$

the reduced Hamiltonian is defined as

$$h(q', p', t) = I_1(E, y, p_y, -\phi_1) \quad (5.3)$$

where we have set  $q' = y$ ,  $p' = p_y$  and  $t = -\phi_1$ . The equations of motion are

$$\begin{aligned} \dot{q}' &= \frac{\partial h}{\partial p'} \\ \dot{p}' &= -\frac{\partial h}{\partial q'} \end{aligned} \quad (5.4)$$

with

$$h(q', p', t) = h(q', p', t+2\pi) \quad , \quad (5.5)$$

and the Poincaré map  $P$  is the mapping of the  $(q', p')$  plane on itself defined as

$$P: (q'(t), p'(t)) \rightarrow (q'(t+2\pi), p'(t+2\pi)) \quad , \quad (5.6)$$

with  $q'(t), p'(t)$  solutions of (5.4). It is an area preserving map possessing all the symmetries of the reduced Hamiltonian. And the Jacobian of its linear approximation is the monodromy matrix.

Of course, we could have used the projection  $\Gamma_2$  of the periodic trajectory onto the plane  $(y, p_y)$  (figure 17b) and defined the reduced Hamiltonian  $I_2(E, x, p_y, -\varphi_2)$ . The choice of a particular reduced Hamiltonian is in general a matter of convenience. In the case of the vertical harmonic oscillation (family V) we must use the projection  $\Gamma_2$  as the projection.  $\Gamma_1$  is a point.

The intersection of the periodic trajectory with the plane  $(q', p')$  is a fixed point of  $P^k$ ,  $k \geq 1$ . At period  $k$ -upling bifurcation points  $(E_b, \tau_b)$  new fixed points of  $P^k$  will appear corresponding to the bifurcated trajectories.

It is convenient to change from coordinates  $(q', p')$  to coordinates  $(q, p)$  so that for any given periodic family the

origin  $(0,0)$  will be the fixed point corresponding to the trajectory of energy  $E_b$  and period  $\tau_b$ . In terms of  $(q, p)$  the reduced Hamiltonian (5.3) can be written<sup>11</sup> as

$$h(q, p, t) = h_0 + \frac{\omega}{2} (p^2 + q^2) + \sum_{m=-\infty}^{\infty} \sum_{j_1, j_2=3}^{\infty} K_{j_1, j_2, m} p^{j_1} q^{j_2} e^{imt} \quad , \quad (5.7)$$

where  $h_0 = \text{constant}$  is the reduced energy of the fixed point trajectory and  $\omega = \alpha/2\pi$  (see (2.28)) is a rational number as discussed in the end of section 2.

The method of Meyer<sup>7</sup> consists of obtaining the fixed points of  $P^k$  at a period  $k$ -upling bifurcation point using in its vicinity the lowest order terms of the expansion of  $P$ . For  $k \geq 3$  the normal form<sup>11</sup> expansion for  $P$  is used while for  $k=1,2$  is used the expansion in powers of  $p$  and  $q$ . We use the same technique of Meyer<sup>7</sup> imposing the existing reflexion symmetries. If  $R$  is a reflexion symmetry (i.e.  $R^2 = 1$ ) of  $P$ , then

$$P^{-1} = RPR \quad . \quad (5.8)$$

This is illustrated in figure 18.

If a canonical transformation  $U$  is performed

$$(p, q) \rightarrow (\tilde{p}, \tilde{q}) \quad ,$$

the transformed Poincaré map is

$$\bar{P} = U^{-1} P U$$

which will have the generalized reflexion symmetry

$$\bar{R} = U^{-1} R U$$

Therefore, canonical transformations conserve the number of reflexion symmetries of the Poincaré map. Moreover,  $\bar{R} \rightarrow R$  at the fixed point.

We shall first consider the case of a single reflexion symmetry and then the case of two reflexion symmetries. In the end we consider the period  $k$ -upling bifurcations,  $k \geq 3$ , of the vertical (harmonic) family which is a special case.

Given the map

$$\begin{pmatrix} q_1 \\ p_1 \end{pmatrix} = P \begin{pmatrix} q_0 \\ p_0 \end{pmatrix}, \quad (5.9)$$

if we take as reflexion symmetry

$$R = \begin{pmatrix} 1 & 0 \\ 0 & -1 \end{pmatrix},$$

the invariance condition (5.8) can be written as

$$P \begin{pmatrix} q_1 \\ -p_1 \end{pmatrix} = \begin{pmatrix} q_0 \\ -p_0 \end{pmatrix}. \quad (5.10)$$

The area preserving condition for (5.9) is

$$\frac{\partial q_1}{\partial q_0} \frac{\partial p_1}{\partial p_0} - \frac{\partial q_1}{\partial p_0} \frac{\partial p_1}{\partial q_0} = 1. \quad (5.11)$$

The linear part of  $P$  will be denoted by  $P_\ell$  (its Jacobian is the monodromy matrix<sup>3</sup>) and we now prove

Proposition 5.1 - Let  $P$  be a Poincaré map possessing one reflexion symmetry. If  $P_\ell$  has only unit eigenvalues, the bifurcations are of types (a) and (b) in Table 1.

Proof - Up to second order, (5.9) can be written as

$$\begin{aligned} q_1 &= q_0 + A p_0 + \varepsilon (a_0 + a_1 q_0 + a_2 p_0) + a_{11} q_0^2 + a_{12} p_0 q_0 + a_{22} p_0^2 \\ p_1 &= p_0 + B q_0 + \varepsilon (b_0 + b_1 q_0 + b_2 p_0) + b_{11} q_0^2 + b_{12} p_0 q_0 + b_{22} p_0^2 \end{aligned} \quad (5.12)$$

where  $\varepsilon$  is the energy parameter introduced in section 4 ( $E = E_D + \varepsilon$ ).

Area preservation condition (5.11) implies that  $AB = 0$ . This will be satisfied if either (i)  $A = 0$  or (ii)  $B = 0$ . As the parameter  $\varepsilon$  is varied, case (ii) gives rise to the generic isochronous bifurcation (4) and (i) to bifurcations of type (b) in Table 1.

(i)  $A = 0$ ,  $B \neq 0$

In this case, the symmetry condition (5.10) together with area preservation imply that  $a_1 = \frac{a_2}{2} + \frac{a_{12}b_0}{2}$ ,  $b = b_1 = a_2/2$ ,  $a_{11} = -b_{22} = a_{12}/2$ ,  $a_{22} = b_{12} = b_{11} = 0$ . Without any loss of generality we set  $B = 1$  and  $b_1 = 1/2$  and the map (5.12) is then given by

$$q_1 = q_0 + (\varepsilon + a_{12}q_0)(p_0 + q_0/2) + \frac{\varepsilon}{2} b_0 a_{12} q_0 + O(\varepsilon^2) \quad (5.13)$$

$$p_1 = p_0 + q_0 + \frac{\varepsilon}{2} (p_0 + q_0 + 2b_0) - \frac{a_{12}}{2} p_0^2 + O(\varepsilon^2)$$

We look for nontrivial fixed points of  $P(q(\varepsilon), p(\varepsilon))$  such that

$$(q(\varepsilon), p(\varepsilon)) \xrightarrow{\varepsilon \rightarrow 0} (0, 0)$$

So we make in (5.13) the following substitution

$$p_i = \sqrt{\varepsilon} t_i \quad (5.14)$$

$$q_i = \varepsilon r_i, \quad i = 0, 1$$

obtaining

$$r_1 = r_0 + \sqrt{\varepsilon} (a_{12} r_0 t_0 + a_{33} t_0^3 + t_0) + O(\varepsilon) \quad (5.15)$$

$$t_1 = t_0 + \sqrt{\varepsilon} (r_0 - \frac{a_{12}}{2} t_0^2 + b_0) + O(\varepsilon)$$

In the above expression the term in  $p_0^3$  has been included because it is of order  $\sqrt{\varepsilon}$ .

Defining the functions

$$\begin{aligned} f(r, t, \varepsilon) &= \frac{r_1 - r_0}{\sqrt{\varepsilon}} \\ g(r, t, \varepsilon) &= \frac{t_1 - t_0}{\sqrt{\varepsilon}} \end{aligned} \quad (5.16)$$

the fixed points of (5.15) are solutions of

$$f(r, t, \varepsilon) = 0$$

$$g(r, t, \varepsilon) = 0$$

The implicit function<sup>3</sup> theorem applied to functions  $f$  and  $g$  guarantees the existence of functions  $r(\varepsilon)$  and  $t(\varepsilon)$  such that

$$f(r(\varepsilon), t(\varepsilon), \varepsilon) = 0$$

$$g(r(\varepsilon), t(\varepsilon), \varepsilon) = 0$$

with

$$r(0) = -b_0$$

$$t(0) = 0 \quad (5.17)$$

or

$$r(0) = (a_{12} - b_0(a_{12}^2 + 2\eta))/2\eta \quad (5.18)$$

$$t(0) = \pm (\xi/\eta)^{1/2},$$

where

$$\eta = -(a_{12}^2 + 2a_{33})/2,$$

$$\xi = 1 - a_{12}b_0.$$

Thus  $(r(0), t(0))$  are the fixed points of (5.15) with (5.17) corresponding to the bifurcating trajectory and (5.18) to the bifurcated trajectories. Correspondingly, the fixed points of (5.13) are

$$q(\epsilon) = -b_0\epsilon, \quad (5.19)$$

$$p(\epsilon) = 0,$$

and

$$q(\epsilon) = \epsilon(a_{12} - b_0(a_{12}^2 + 2\eta))/2\eta, \quad (5.20)$$

$$p(\epsilon) = \pm (\epsilon\xi/\eta)^{1/2}.$$

The eigenvalues of the Jacobian of (5.13) calculated at the fixed point (5.19) are

$$\lambda = 1 \pm \sqrt{\xi\epsilon} + O(\epsilon) \quad (5.21)$$

and at the fixed points (5.20) are

$$\bar{\lambda} = 1 \pm \sqrt{-2\xi\epsilon} + O(\epsilon). \quad (5.22)$$

Now, assuming  $\xi > 0$ , if  $\eta > 0$ , for  $\epsilon < 0$  only the fixed point (5.19) exists and it is stable (see (5.21)); for  $\epsilon > 0$  there exist the fixed point (5.19) now unstable (see (5.21)) and the two fixed points (5.20) that are stable (see (5.22)).

For  $\xi < 0$ , if  $\eta < 0$ , for  $\epsilon < 0$  only the fixed point (5.19) exists and it is unstable; for  $\epsilon > 0$  there exist the fixed point (5.19), stable, and the two fixed points (5.20), unstable.

These bifurcations correspond to case (b) presented in Table 1 and the second part of the proposition is proved.

Remark - For  $\xi > 0$ ,  $\eta < 0$  and  $\xi < 0$ ,  $\eta > 0$  we obtain the same type of bifurcations with the bifurcated trajectories existing for  $\epsilon < 0$ .

(ii)  $B = 0$ ,  $A \neq 0$

In this case, the reflexion symmetry condition (5.10) together with area preservation imply that  $b_1 = 2a_1 - 2a_0(a_{12} - a_{11})$ ,  $b_2 = b_1 - a_1$ ,  $b_{11} = b_{12} = 2a_{11}$ ,  $a_{12} = 4a_{22}$ ,  $b_{22} = a_{11} - 2a_{22}$  and  $a_0 = b_0/2$ . Without any loss of generality we set  $A = 1$  and  $a_1 = 1$  and the map (5.12) is given by

$$q_1 = q_0 + p_0 + \epsilon(q_0 + a_2 p_0 + b_0/2) + 4a_{22} p_0 q_0 + a_{11} q_0^2 + a_{22} p_0^2 + O(\epsilon^2) ,$$

$$(5.23)$$

$$p_1 = p_0 + (b_1 q_0 + b_2 p_0 + b_0) + 2a_{11} q_0 (p_0 + q_0) + (a_{11} - 2a_{22}) p_0^2 + O(\epsilon^2) .$$

We now make the substitution

$$q_i = \sqrt{\epsilon} r_i ,$$

$$p_i = \sqrt{\epsilon} t_i , \quad i = 0, 1$$

$$(5.24)$$

obtaining

$$r_1 - r_0 = t_0 + \sqrt{\epsilon} \left[ \frac{b_0}{2} + 4a_{22} r_0 t_0 + a_{11} r_0^2 + a_{22} t_0^2 \right] + O(\epsilon) ,$$

$$(5.25)$$

$$t_1 - t_0 = \sqrt{\epsilon} (b_0 + 2a_{11} r_0 t_0 + 2a_{11} r_0^2 + (a_{11} - 2a_{22}) t_0^2) + O(\epsilon) .$$

From the implicit function theorem the fixed points of (5.24) are

$$r_{\pm}(0) = \pm (-b_0/2a_{11})^{1/2} ,$$

$$t(0) = 0 .$$

Correspondingly, the fixed points of (5.23) are (see (5.24))

$$q_{\pm}(\epsilon) = \pm (-\epsilon b_0/2a_{11})^{1/2} ,$$

$$p(\epsilon) = 0 .$$

$$(5.26)$$

The eigenvalues of the Jacobian of (5.23) at  $(q_{\pm}(\epsilon), 0)$  are

$$\lambda_{+} = 1 \pm 2(-\epsilon a_{11} b_0/2)^{1/4} ,$$

$$(5.27)$$

and at  $(q_{-}(\epsilon), 0)$  are

$$\lambda_{-} = 1 \pm i2(-\epsilon a_{11} b_0/2)^{1/4} .$$

$$(5.28)$$

Thus, if  $a_{11} b_0 < 0$  ( $a_{11} b_0 > 0$ ) no fixed point exists for  $\epsilon < 0$  ( $\epsilon > 0$ ) while for  $\epsilon > 0$  ( $\epsilon < 0$ ) there exist two fixed points: one unstable (5.27) and one stable (5.28). The case  $a_{11} b_0 < 0$  corresponds to a minimum in the  $\epsilon \times r$  plot at  $\epsilon = 0$  and  $a_{11} b_0 > 0$  corresponds to a maximum. This is the generic type of bifurcation (4) corresponding to case (a) in Table 1. And the proof of proposition 5.1 is completed.

We now consider the period doubling bifurcation. In fact, if the bifurcating trajectory has only one reflexion symmetry, the generic type of bifurcation is obtained. This is the content of



**Proposition 5.2** - Let  $P$  be a Poincaré map having one reflexion symmetry. If  $P_\varepsilon$  has eigenvalues  $-1$  the bifurcations are of type (a) presented in Table 2 (generic or symmetry preserving).

**Proof** - Up to second order the map  $P$  is given by

$$\begin{aligned} q_1 &= -q_0 + Ap_0 + \varepsilon(a_0 + a_1 q_0 + a_2 p_0) + a_{11} q_0^2 + \\ &+ a_{12} q_0 p_0 + a_{22} p_0^2 + \dots \\ p_1 &= -p_0 + Bq_0 + \varepsilon(b_0 + b_1 q_0 + b_2 p_0) + b_{11} q_0^2 + \\ &+ b_{12} q_0 p_0 + b_{22} p_0^2 + \dots \end{aligned} \quad (5.29)$$

Again, area preservation implies  $A \cdot B = 0$ . We shall consider only case  $A = 0$  as  $B = 0$  gives the same results.

The symmetry condition (5.10) together with area preservation imply  $b_1 = a_2 = 2a_1$ ,  $b_2 = -a_2/2$ ,  $a_{11} = a_{22} = -b_{12} = -a_{12} = -2b_{22} = 4b_{11}$  and  $b_0 = -a_0/2$ . Without loss of generality we choose  $a_2 = B = 1$  and (5.29) reduces to

$$\begin{aligned} q_1 &= -q_0 + \varepsilon(p_0 - q_0/2 + q_0) + a_{12}(p_0 q_0 - q_0^2 + p_0^2) + O(\varepsilon^2), \\ p_1 &= -p_0 + q_0 + \frac{\varepsilon}{2}(2q_0 - p_0 - a_0) + a_{12}(p_0 q_0 - q_0^2/4 + p_0^2/2) + \\ &+ O(\varepsilon^2) \end{aligned} \quad (5.30)$$

Making the substitution

$$\begin{aligned} q_i &= \varepsilon r_i, \\ p_i &= \sqrt{\varepsilon} t_i, \quad i = 0, 1, \end{aligned} \quad (5.31)$$

we obtain

$$\begin{aligned} r_1 &= -r_0 + (a_0 - a_{12} t_0^2) + \sqrt{\varepsilon}(t_0 + a_{12} r_0 t_0 + a_{33} t_0^3) + O(\varepsilon), \\ t_1 &= -t_0 + \sqrt{\varepsilon} \left( r_0 + \frac{a_{12}}{2} t_0^2 - \frac{a_0}{2} \right) + O(\varepsilon) \end{aligned} \quad (5.32)$$

And the map

$$\begin{pmatrix} r_2 \\ t_2 \end{pmatrix} = p^2 \begin{pmatrix} r_0 \\ t_0 \end{pmatrix}$$

is then given by

$$\begin{aligned} r_2 &= r_0 - 2\sqrt{\varepsilon} t_0 (1 + a_{33} t_0^2 - a_{12} r_0 - a_{12}^2 t_0^2 + a_0 a_{12}) + O(\varepsilon), \\ t_2 &= t_0 - 2\sqrt{\varepsilon} \left( r_0 + \frac{a_{12}}{2} t_0^2 - \frac{a_0}{2} \right) + O(\varepsilon) \end{aligned} \quad (5.33)$$

From the implicit function theorem<sup>3</sup> the fixed points of  $p^2$  (5.33) are

$$\begin{aligned} r(0) &= a_0/2, \\ t(0) &= 0, \end{aligned} \quad (5.34)$$

and

$$\begin{aligned} r(0) &= \left[ a_0(a_{33} - a_{12}^2) + a_{12} \right] / \delta, \\ t(0) &= \pm (-2\zeta/\delta)^{1/2}, \end{aligned} \quad (5.35)$$

where

$$\begin{aligned} \delta &\equiv 2a_{33} - a_{12}^2, \\ \zeta &\equiv 1 + a_{12}a_0/2. \end{aligned}$$

The fixed point given by (5.34) is also a fixed point of (5.32) therefore it corresponds to a periodic trajectory that has half the period of the trajectory corresponding to the fixed point (5.35).

The eigenvalues of the Jacobian of (5.32), calculated at the fixed point (5.34) are

$$\lambda = -1 \pm (\zeta\epsilon)^{1/2} + O(\epsilon), \quad (5.36)$$

and the eigenvalues of the Jacobian of (5.33), calculated at the fixed point (5.35) are

$$\bar{\lambda} = 1 \pm 2(-2\zeta\epsilon)^{1/2} + O(\epsilon). \quad (5.37)$$

Thus, if  $\zeta > 0$  ( $\zeta < 0$ ) the fixed point (5.34) will switch from stable to unstable as  $\epsilon$  varies from negative

(positive) to positive (negative) values (see (5.36)). Moreover if  $\delta\zeta < 0$  the fixed point (5.35) will exist only for  $\epsilon > 0$  (see (5.31)) and it is stable if  $\zeta > 0$  and unstable if  $\zeta < 0$ . This is the generic period doubling bifurcation corresponding to cases (a) in Table 2. And proposition 5.2 is demonstrated.

Remark - If  $\delta\zeta > 0$  we obtain the same kind of bifurcation with the period doubled solution existing only for  $\epsilon < 0$ .

In order to examine the period  $k$ -upling bifurcations,  $k \geq 3$ , we have to express the reduced Hamiltonian (5.7) in its normal form<sup>2,11</sup>. This is achieved by making successive time dependent canonical transformations which eliminate the time dependence of (5.7) up to an order  $N$ . The period  $k$ -upling bifurcations occur at rational values of  $\omega$  therefore we have to use the resonant form. Introducing the variables

$$\begin{aligned} J &= \frac{p^2 + q^2}{2}, \\ \vartheta &= \tan^{-1} \frac{p}{q}, \end{aligned} \quad (5.38)$$

and writing

$$\omega = \frac{l}{k} + \epsilon, \quad l \text{ and } k \text{ non-commensurate integers}, \quad (5.39)$$

the resonant normal form<sup>2,11</sup> of (5.7) is obtained from the

resonance condition  $\frac{\ell}{k} (j_1 - j_2) = m$  (see Appendix). The result is

$$h(J, \vartheta, t) = \epsilon J + \sum_{j=2}^{k/2} C_j J^j + a J^{k/2} \sin(k\vartheta) + b J^{k/2} \cos(k\vartheta) + \dots \quad (5.40)$$

the time dependence lying in higher order terms (we have set  $h_0 = 0$ ).

The equations of motion, up to order  $k/2$ , are

$$\dot{J} = -\frac{\partial h}{\partial \vartheta} = a k J^{k/2} \cos(k\vartheta) + b k J^{k/2} \sin(k\vartheta) \quad (5.41)$$

$$\dot{\vartheta} = \frac{\partial h}{\partial J} = \epsilon + \sum_{j=2}^{k/2} C_j j J^{j-1} + a \frac{k}{2} J^{k/2-1} \sin(k\vartheta) + b \frac{k}{2} J^{k/2-1} \cos(k\vartheta)$$

And the map,

$$\begin{pmatrix} J_1 \\ \vartheta_1 \end{pmatrix} = P \begin{pmatrix} J_0 \\ \vartheta_0 \end{pmatrix} \quad (5.42)$$

is obtained by integrating (5.41) from 0 to  $2\pi$  in the approximation  $J = J_0$ ,  $\vartheta = \vartheta_0$ :

$$\begin{aligned} J_1 &= J_0 - 2\pi k a J_0^{k/2} \cos(k\vartheta_0) + 2\pi k b J_0^{k/2} \sin(k\vartheta_0) \quad (5.43) \\ \vartheta_1 &= \vartheta_0 + 2\pi\epsilon + \sum_{j=1}^{k/2-1} 2\pi(j+1)C_j J_0^j + \pi k a J_0^{k/2-1} \sin(k\vartheta_0) + \\ &\quad + \pi k b J_0^{k/2-1} \cos(k\vartheta_0) \end{aligned}$$

We now impose one reflexion symmetry on the map.

In the variables  $(J, \vartheta)$  the reflexion symmetry condition (5.10) becomes (see (5.38))

$$P \begin{pmatrix} J_0 \\ -\vartheta_1 \end{pmatrix} = \begin{pmatrix} J_0 \\ -\vartheta_0 \end{pmatrix} \quad (5.44)$$

which imposed on (5.43) gives  $a = 0$  so that (5.43) reduces to

$$\begin{aligned} J_1 &= J_0 + 2\pi k b J_0^{k/2} \sin(k\vartheta_0) \quad (5.45) \\ \vartheta_1 &= \vartheta_0 + 2\pi\epsilon + \sum_{j=1}^{k/2-1} 2\pi(j+1)C_j J_0^j + \pi k b J_0^{k/2-1} \cos(k\vartheta_0) \end{aligned}$$

So we now state

**Proposition 5.3** - Let  $P$  be a Poincaré map having one reflexion symmetry. If its linear approximation  $P_\ell$  has eigenvalues  $e^{\pm 2\pi i \ell/k}$ ,  $\ell$  and  $k$  noncommensurate integers,  $\ell < k$  and  $k \geq 3$ ,

then it exhibits period k-upling bifurcations of generic type corresponding to cases (a) in Tables 3, 4 and 5.

Proof - We shall omit it because it follows the proof of proposition 5.4 given below for the case of two reflexion symmetries.

We now consider the case of two reflexion symmetries, i.e., the bifurcations of symmetric librations.

Remark - We have not obtained the fixed points of the isochronous and period doubling bifurcations when the trajectory is a symmetric libration ( $4^2$  and  $Z^2$ ). In this case it may or may not lose one of its reflexion symmetries when undergoing an isochronous bifurcation but it always loses one of them when undergoing a period-doubling bifurcation (cases b and c in Table 1 and b in Table 2).

We shall analyse the period k-upling bifurcations,  $k \geq 3$ , of symmetric librations. For the reduced Hamiltonian (5.7), the symmetry  $x \rightarrow -x$  is imposed by replacing  $m$  by  $2m$  since this symmetry corresponds to invariance of  $h(q,p,t)$  when  $t \rightarrow t + \pi$ :

$$h(q,p,t) = \omega \left( \frac{p^2 + q^2}{2} \right) + \sum_{m=-\infty}^{\infty} \sum_{j_1 + j_2 = 3}^{\infty} K_{j_1 j_2 m} p^{j_1} q^{j_2} e^{i2mt} \quad (5.46)$$

Now, the resonant normal form of (5.46) depends on

$k$  being even or odd as the resonance condition is  $\frac{\omega}{k}(j_1 - j_2) = 2m$ .

If  $k$  is odd, the lowest order normal form expansion for the reduced Hamiltonian is

$$h(J, \vartheta, t) = \epsilon J + \sum_{j=2}^{k/2} C_j J^j + b J^{k/2} \cos(k\vartheta) + \dots \quad (5.47)$$

or

$$h(J, \vartheta, t) = \epsilon J + \sum_{j=2}^k C_j J^j + b J^k \cos(2k\vartheta) + \dots \quad (5.48)$$

If  $k$  is even only form (5.48) is possible.

The map (5.42) is obtained as previously, by integrating the equations of motion in the approximation  $J = J_0$ ,  $\vartheta = \vartheta_0$ . The reduced Hamiltonian given by (5.47), valid for  $k$  odd, will produce the map given by (5.45) possessing one reflexion symmetry. And the reduced Hamiltonian given by (5.48) leads to the map (valid for  $k$  even or odd)

$$\begin{aligned} J_1 &= J_0 + 2\pi k b J_0^k \sin(2k\vartheta_0) \\ \vartheta_1 &= \vartheta_0 + 2\pi\epsilon + \sum_{j=1}^{k-1} 2\pi(j+1) C_j J_0^j + \pi k b J_0^{k-1} \cos(2k\vartheta_0) \end{aligned} \quad (5.49)$$

We shall now prove

Proposition 5.4 - Let  $P$  given by (5.42) be a Poincaré map possessing two reflexion symmetries (corresponding to a symmetric libration). If the eigenvalues of the monodromy matrix are given by  $e^{\pm 2\pi i \ell/k}$ ,  $k \geq 3$ ,  $\ell < k$  ( $\ell$  and  $k$  noncommensurate integers) then it exhibits period  $k$ -upling bifurcations. If  $k$  is even it is of type (b) in Table 5 and if  $k$  is odd it may be either of type (a) (generic case) or type (b) of Tables 3 and 5.

Proof - If  $k$  is odd, one of the possible lowest order normal form expression for the map is (5.45) therefore, from proposition 5.3 it follows that the bifurcations are of the generic type (case (a) in Tables 3 and 5). In the case of expansion (5.49) (which is valid for  $k$  even or odd) in order to find the non-trivial fixed points of  $P^k$  we make the substitution

$$J = R\epsilon \tag{5.50}$$

so that

$$R_1 - R_0 = 2\pi k b \epsilon^{k-1} R_0^k \sin(2k\phi_0) + O(\epsilon^k) \tag{5.51}$$

$$\phi_1 - \phi_0 = 2\pi\epsilon(1 + 2C_1 R_0) + O(\epsilon^2)$$

and

$$R_k - R_0 = 2\pi k^2 b \epsilon^{k-1} R_0^k \sin(2k\phi_0) + O(\epsilon^k) \tag{5.52}$$

$$\phi_k - \phi_0 = 2\pi\epsilon(1 + 2kC_1 R_0) + O(\epsilon^2)$$

And from the implicit function theorem the fixed points of  $P^k$  (5.52) are

$$\begin{aligned} R(0) &= -\frac{1}{2kC_1} \\ \phi_{2n}^{(+)} &= \frac{2n\pi}{k} \\ \phi_{2n-1}^{(+)} &= (2n-1)\frac{\pi}{k} \\ \phi_{2n}^{(-)} &= (2n + \frac{1}{2})\frac{\pi}{k} \\ \phi_{2n-1}^{(-)} &= (2n - \frac{1}{2})\frac{\pi}{k} \end{aligned} \tag{5.53}$$

with  $n = 1, 2, \dots, k$ .

Therefore at  $\epsilon = 0$ , besides the point  $(0,0)$ ,  $P^k$  has four sets of  $k$  fixed points given in (5.53), each set corresponding to a periodic trajectory of period  $k\tau_b$ . Their stability is obtained calculating the trace of the Jacobian of (5.52) at the fixed points, imposing area preservation:

$$\text{tr} \left. \frac{\partial(R_k, \phi_k)}{\partial(R_0, \phi_0)} \right|_{(\phi^{(\pm)}, R(0))} = 2 \pm (2\pi k)^4 b C_1 \epsilon^k \left(-\frac{1}{2kC_1}\right)^k + O(\epsilon^{k+1}) \tag{5.54}$$

Therefore if the sets of fixed points  $(R(0), \phi_{2n}^{(+)})$ ,  $(R(0), \phi_{2n-1}^{(+)})$  are stable, then  $(R(0), \phi_{2n}^{(-)})$  and  $(R(0), \phi_{2n-1}^{(-)})$

are unstable and vice-versa. This corresponds to the type (b) of bifurcation presented in Tables 3 and 5. And the proposition is proved.

We now analyse the bifurcations of the harmonic  $V$  family. As already mentioned, in this case we have to use the reduced Hamiltonian  $I_2$  which will then map the plane  $(x, p_x)$  on itself (see figure 17a). Therefore, the Poincaré map in this case is obtained by imposing the symmetry  $q \rightarrow -q$  ( $x \rightarrow -x$ ) on (5.45) which already has the symmetry  $p \rightarrow -p$ . In terms of variable  $\vartheta$  this symmetry condition is

$$P \begin{pmatrix} I_1 \\ \pi - \vartheta_1 \end{pmatrix} = \begin{pmatrix} I_0 \\ \pi - \vartheta_0 \end{pmatrix} \quad (5.55)$$

And we must consider two cases:  $k$  even and  $k$  odd.

If  $k$  is even the map is given by (5.45) which already satisfies condition (5.55).

If  $k$  is odd condition (5.55) is satisfied only if  $b = 0$  so that higher order terms must be considered in the reduced Hamiltonian. Up to terms of order  $k$  it is given by

$$h(I, \vartheta, t) = \epsilon J + \sum_{j=2}^k C_j J^j + b J^k \cos(2k\vartheta) \quad , \quad (5.56)$$

and the map in the lowest order approximation is given by (5.49) which automatically satisfies condition (5.55).

It is now easy to prove the

Lemma - Given a vertical periodic trajectory, if its monodromy matrix has eigenvalues  $e^{\pm 2\pi i \ell / k}$ ,  $k > 3$ ,  $\ell < k$  ( $\ell$  and  $k$  noncommensurate integers) then it exhibits period  $k$ -upling bifurcation. If  $k$  is even the bifurcation is generic (types (a) of Tables 4 and 5). If  $k$  is odd then the bifurcations are of the type given in Table 6 (which is the same as type (b) in Tables 3-5).

The proof is immediate since if  $k$  is even the map is given by (5.45) and from proposition 5.3 the bifurcation is of the generic type. Now, if  $k$  is odd, the map is given by (5.49) and from proposition 5.4 the bifurcations are of the type shown in Table 6.

#### ACKNOWLEDGEMENTS

Two people were important in the inception of this project, Emerson J.V. de Passos and Marcos Saraceno and we thank them most heartily. Two of us (M.A.M. de Aguiar and C.P. Malta) would like to thank Alfredo M. Ozorio de Almeida for the frequent discussions that were invaluable for the classification of all possible branchings in Hamiltonians possessing symmetries. Marta L.C. Rabello was involved in the early days and lent her name to the potential.

Financial support in Brazil came from FAPESP (Fundação de Amparo à Pesquisa do Estado de São Paulo) and CNPq (Conselho Nacional de Desenvolvimento Científico e Tecnológico). In USA it came from the Department of Energy (DOE) under contracts \*DE-AC02-76ER03069 and \*DE-AC05-84OR21400, and from the National Science Foundation under grant \*INT-82/2846.

#### APPENDIX

We give here a sketchy derivation of the normal form expansion<sup>2,11</sup> for the Hamiltonian given in (5.7). In terms of

$$\begin{aligned} z &= p + iq \\ \bar{z} &= p - iq \end{aligned} ,$$

the reduced Hamiltonian expansion (5.7) is

$$-2ih(z, \bar{z}, t) = -i\omega z\bar{z} + \sum_{m=-\infty}^{\infty} \sum_{j_1+j_2=3}^{\infty} K_{j_1 j_2 m} z^{j_1} \bar{z}^{j_2} e^{imt} ,$$

with  $K_{j_1 j_2 m} = -\bar{K}_{j_2 j_1 -m}$  to ensure reality of  $h$  (we have set  $h_0 = 0$ ).

Through the time dependent canonical transformation generated by

$$S(z, \bar{z}) = z\bar{z} + \sum_{m=-\infty}^{\infty} \sum_{j_1+j_2=3}^{\infty} S_{j_1 j_2 m} S_{j_1 j_2 m} z^{j_1} \bar{z}^{j_2} e^{imt} ,$$

the Hamiltonian in the new variables is given by

$$\begin{aligned} -2ih(z, \bar{z}, t) &= -i\omega z\bar{z} + \sum_{m=-\infty}^{\infty} \left\{ K_{j_1 j_2 m} + \right. \\ &\left. + i \left[ \omega(j_1 - j_2) - m \right] S_{j_1 j_2 m} \right\} z^{j_1} \bar{z}^{j_2} e^{imt} + \text{Higher order terms (HOT)} . \end{aligned}$$

Thus, if  $\omega(j_1 - j_2) - m \neq 0$  (i.e.,  $\omega$  irrational), the time dependence in the lower order terms may be eliminated by choosing

$$S_{j_1 j_2 m} = \frac{i K_{j_1 j_2 m}}{m - \omega(j_1 - j_2)}$$

The only term that could remain for irrational  $\omega$  is the term  $m=0$  and  $j_1 = j_2$ . Therefore, for irrational  $\omega$ , through successive time dependent canonical transformation the reduced Hamiltonian can be cast in the form

$$-2ih(z, \bar{z}, t) = -i\omega z\bar{z} + \sum_{j=2}^{N/2} K_{jj0} (z\bar{z})^j + \text{HOT}(z, \bar{z}, t)$$

to any desired order  $N$ . In the original variables it is

$$h(q, p, t) = \omega \left( \frac{p^2 + q^2}{2} \right) + \sum_{j=2}^{N/2} c_j \left( \frac{p^2 + q^2}{2} \right)^j + \text{HOT}(q, p, t)$$

Now, if  $\omega$  is rational,  $\omega = \frac{\ell}{k}$ , the above expansion is not valid as it is not possible to eliminate the terms of order  $k$  that satisfy the resonance condition

$$\frac{\ell}{k} (j_1 - j_2) - m = 0$$

So we have

$$-2ih(z, \bar{z}, t) = -i\omega z\bar{z} + \sum_{j=2}^{k/2} K_{jj0} (z\bar{z})^j + K_{k0\ell} z^k e^{i\ell t} + K_{0k-\ell} e^{-i\ell t} + \text{HOT}(z, \bar{z}, t)$$

The resonant terms cannot be eliminated but its time dependence may be eliminated. We set  $\omega = \frac{\ell}{k} + \epsilon$  and make the canonical transformation

$$\zeta = z e^{i\frac{\ell}{k}t}, \quad \bar{\zeta} = \bar{z} e^{-i\frac{\ell}{k}t}$$

which is generated by

$$\sigma = z\bar{\zeta} e^{i\frac{\ell}{k}t}$$

obtaining

$$-2ih(\zeta, \bar{\zeta}, t) = -i\epsilon\zeta\bar{\zeta} - 2i \sum_{j=2}^{k/2} C_j (\zeta\bar{\zeta})^j + 2i\text{Im}(K_{k0\ell} \zeta^k) + \text{HOT}$$

In terms of the real coordinates  $J, \theta$  in (5.38) the expansion is

$$h(J, \theta, t) = \epsilon J + \sum_{j=2}^{k/2} C_j J^j + a J^{k/2} \sin(k\theta) + b J^{k/2} \cos(k\theta) + \text{HOT}$$

with  $K_{k0\ell} = a + ib$ . This expansion is valid at  $\epsilon = 0$ .



REFERENCES

- 1) M.A.M. de Aguiar and C.P. Malta, *J. Chem. Phys.* 84 (1986) 6916.  
A.K. Kerman, S.E. Koonin, *Ann. Phys.* 100 (1976) 332.  
M. Saraceno, *Rev. Bras. Fis., Vol. Esp.* 3 (1982) 248.
- 2) V. Arnold, "Les Méthodes Mathématiques de la Mécanique Classique", Éditions Mir, 1976.
- 3) V.A. Yakubovich and V.M. Starzhinskii, "Linear Differential Equations with Periodic Coefficients", Keter Publishing House, Jerusalem, 1975.  
L. Pontriaguine, "Equations Differentielles Ordinaires", Editions Mir, 1975.
- 4) M. Baranger and K.T.R. Davies, in preparation.
- 5) MARCO:  $V(x,y) = \frac{1}{4} (x^2+y^2-1)^2 + \mu \frac{y}{2} (3-x^2-y^2)$  ,  $\mu = 0.15$   
DELFI:  $V(x,y) = \frac{1}{4} (x^2+y^2)^2 + \frac{1}{4} \mu x^3(y-1) - y(x^2+y^2) +$   
 $+ \frac{1}{2} (x^2+3y^2)$  ,  $\mu = \frac{8}{3} \sqrt{\frac{2}{3}}$   
NELSON:  $V(x,y) = \left(y - \frac{x^2}{2}\right)^2 + \mu \frac{x^2}{2}$  ,  $\mu = 0.1$   
and  
MARTA, given in (1.1).
- 6) M. Baranger and K.T.R. Davies, results for NELSON, in preparation.
- 7) K.R. Meyer, *Trans. Am. Math. Soc.* 149 (1970) 95.
- 8) M. Hénon, *Quarterly of Appl. Math.* 27 (1969) 291.  
M. Hénon and C. Heiles, *Astron. Journal* 69 (1964) 73.

- 9) A libration is a trajectory that is followed on itself in both directions between two end points and a rotation is a trajectory that is followed in one direction only making a closed loop.
- 10) J. Guckenheimer and P. Holmes, "Nonlinear Oscillations, Dynamical Systems and Bifurcations of Vector Fields", Applied Mathematical Sciences Vol. 42, Springer-Verlag, 1983.
- 11) A.M. Ozório de Almeida, "Hamiltonian Systems: Chaos and Quantization", to be published by Cambridge University Press, and "Sistemas Hamiltonianos: Caos e Quantização", to be published by Editora UNICAMP, Campinas.

## TABLE CAPTIONS

Table 1 - Isochronous bifurcations: a) Generic case, the trajectory simply switches from stable to unstable or vice-versa (it occurs at points denoted by  $\bar{4}$  for which  $\text{Tr}M = 4$  and  $\frac{dE}{d\tau} = 0$ ); b) bifurcations with loss of one symmetry and change of stability of the bifurcating trajectory (they occur at points denoted by 4); c) bifurcations with loss of one symmetry with the bifurcating trajectory remaining stable (it occurs at points  $4^2$  where  $\text{Tr}M = 4$  and  $\frac{d \text{Tr}M}{dE} = 0$ ).

Table 2 - Period-doubling bifurcations: a) Generic case (symmetry preserving bifurcation occurring at points denoted by Z); b) bifurcation at  $Z^2$  points, each set of alternating fixed points corresponding to one periodic trajectory.

Table 3 - Period-tripling bifurcations: a) Generic case; b) bifurcation with loss of one symmetry, each set of alternating fixed points corresponding to one periodic trajectory.

Table 4 - Period-quadrupling bifurcations: a) Generic case (notice that a symmetric libration does not exhibit the generic period-quadrupling); b) bifurcation with loss of one symmetry, each set of alternating fixed points corresponding to one trajectory.

Table 5 - Period n-upling bifurcation,  $n \geq 5$ : a) Generic case (notice that  $n$  even does not exhibit the generic case if the bifurcating trajectory is a symmetric libration); b) bifurcation with loss of one symmetry, each set of alternating fixed points corresponding to one periodic trajectory.

Table 6 - V family period n-upling,  $n \geq 3$  odd: the bifurcated trajectories have 1 symmetry (each set of alternating fixed points corresponds to one periodic trajectory).

## FIGURE CAPTIONS

Figure 1 - Equipotential lines of the MARTA potential.

Figure 2 -  $E \times \tau$  plot of the horizontal families.

Figure 3 -  $E \times \tau$  plot of the vertical families.

Figure 4 -  $E \times \tau$  plot for the saddle point families.

Figure 5 -  $TrM \times E$  illustrating the points denoted by  $4$ ,  $4^2$ ,  $z$  and  $z^2$ .

Figure 6 - Detail of the loop  $V2a$ ,  $V2b$  and  $V2aa$  (intentionally enlarged out of scale) in figure 3.

Figure 7 -  $E \times \tau$  plot of the first period-tripling families of the  $V$ -family.

Figure 8 - Detail of the connection of the horizontal and the vertical families by a rotation,  $Va = Hb$ .

Figure 9 - Detail of the  $E \times \tau$  plot of an isolated family showing the shape of an eight (intentionally enlarged out of scale).

Figure 10 -  $E \times \tau$  plot of a group of isolated families.

Figure 11 -  $x$ - $y$  plot of a member of the irregular family  $F$  and a sequence of members of the bifurcated family  $Fa$ .

Figure 12 -  $E \times \tau$  plot of an isolated family of asymmetric rotations (it does not have an isochronous bridge).

Figure 13 -  $x$ - $y$  plot of some trajectories of the  $H$  family superimposed over the equipotential lines of  $V(x,y)$ .

Figure 14 -  $x$ - $y$  plot of some trajectories of the  $S_+$  family superimposed over the equipotential lines of  $V(x,y)$ .

Figure 15 -  $x$ - $y$  plot of member trajectories of the families generated at several bifurcation points of the  $H$  family.

Figure 16 - Detail of the  $E \times \tau$  plot of the period tripled families  $Ha3a$  and  $Ha3b$ .

Figure 17 - (a) Projection onto  $(x, p_x)$  plane of a periodic trajectory having  $x$  and  $t$  reflexion symmetries.  
(b) Projection onto  $(y, p_y)$  plane of a periodic trajectory having  $t$  reflexion symmetry.

Figure 18 - Illustrating the effect of a reflexion symmetry  $R$  on the map  $P$ .

TABLE 1

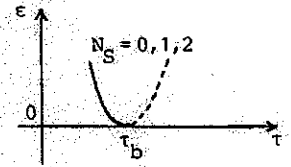

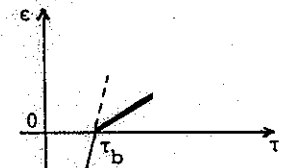
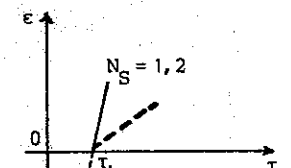



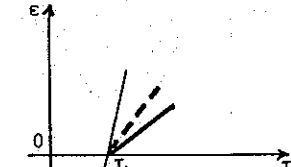


$\epsilon \times \tau$	Fixed points of P	
	$\epsilon < 0$	$\epsilon > 0$
<p>a) Symmetry preserved</p> 		
<p>b) <math>\Delta N_S = -1</math></p>  	  	
<p>c) <math>\Delta N_S = -1</math></p> 		

TABLE 2

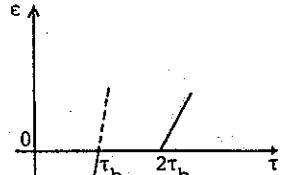
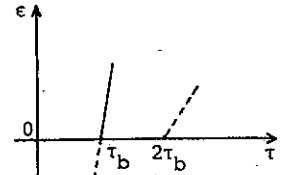



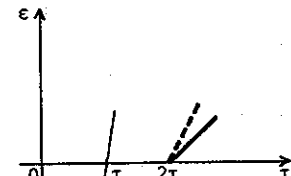


$\epsilon \times \tau$	Fixed points of $P^2$	
	$\epsilon < 0$	$\epsilon > 0$
<p>a) Symmetry preserved</p>  		 
<p>b) <math>\Delta N_S = -1</math></p> 		

TABLE 3

$\epsilon \times \tau$	Fixed points of $P^3$		
	$\epsilon < 0$	$\epsilon = 0$	$\epsilon > 0$
<p>a) Symmetry preserved</p>			
<p>b) <math>\Delta N_S = -1</math></p>			

TABLE 4

$\epsilon \times \tau$	Fixed point of $P^4$		
	$\epsilon < 0$	$\epsilon = 0$	$\epsilon > 0$
<p>a) Symmetry preserved</p>			
<p>b) <math>\Delta N_S = -1</math></p>			

TABLE 5

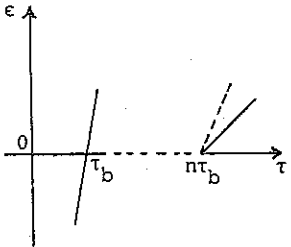

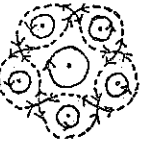
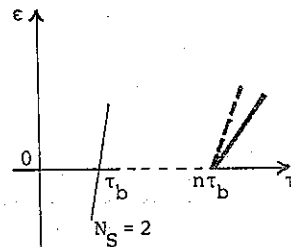

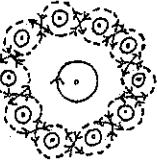
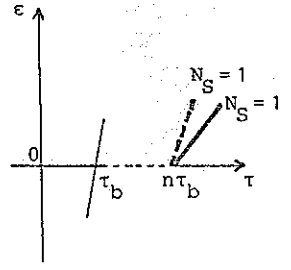

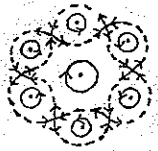
$\epsilon \times \tau$	Fixed points of $P^n$ , $n > 5$	
	$\epsilon < 0$	$\epsilon > 0$
<p>a) Symmetry preserved:</p> $N_S = \begin{cases} 0, 1, 2 & \text{if } n \text{ odd} \\ 0, 1 & \text{if } n \text{ even} \end{cases}$ 		
<p>b) <math>\Delta N_S = -1</math></p> 		

TABLE 6

$\epsilon \times \tau$	Fixed points of $P^n$ , $n > 3$ odd	
	$\epsilon < 0$	$\epsilon > 0$
		

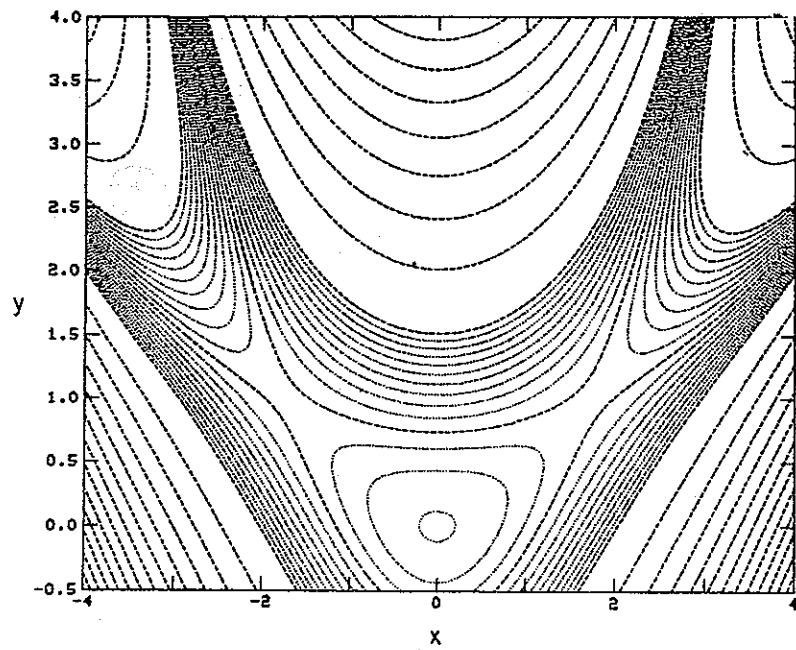


FIGURE 1

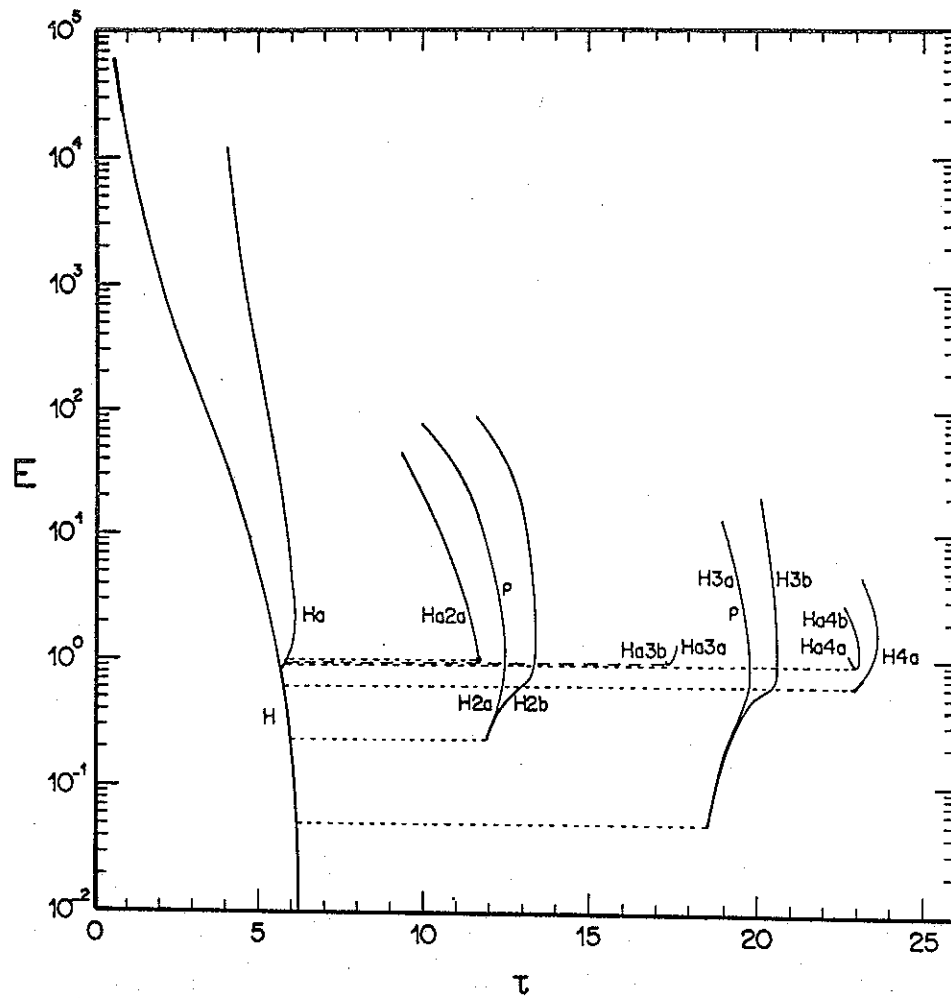


FIGURE 2

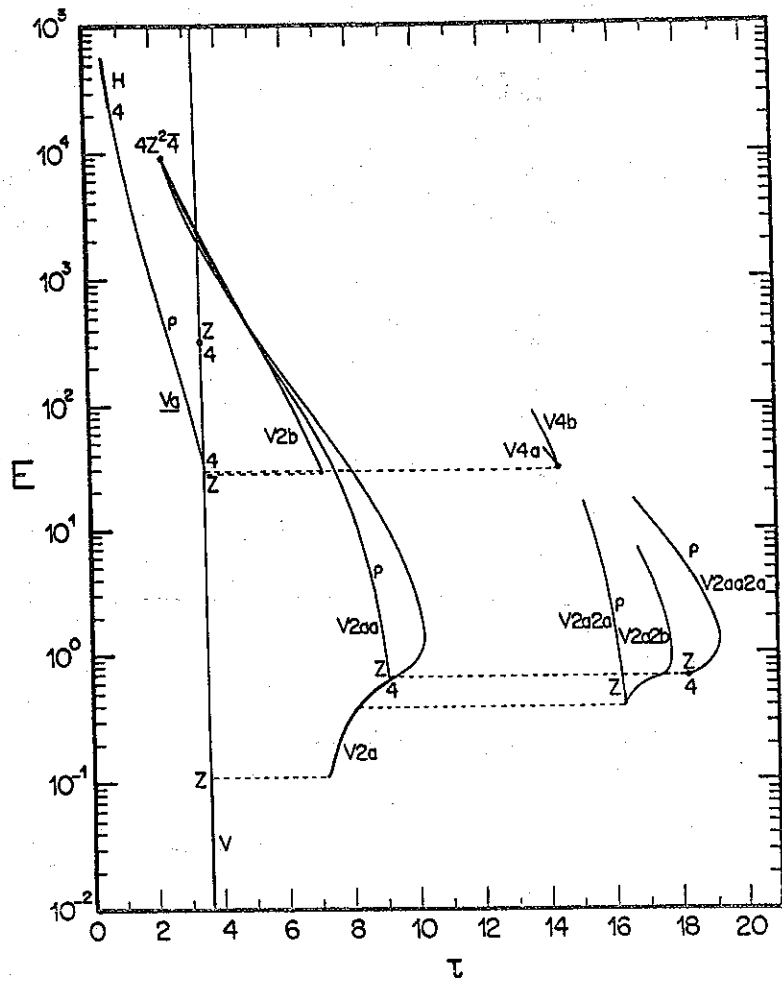


FIGURE 3

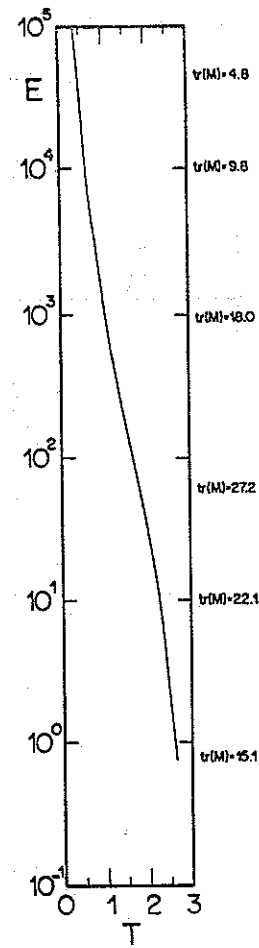


FIGURE 4



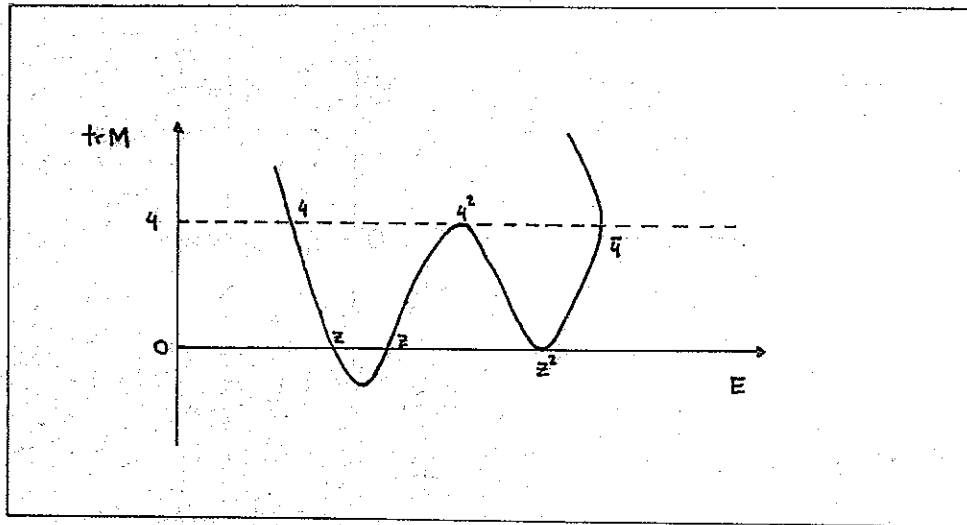


FIGURE 5

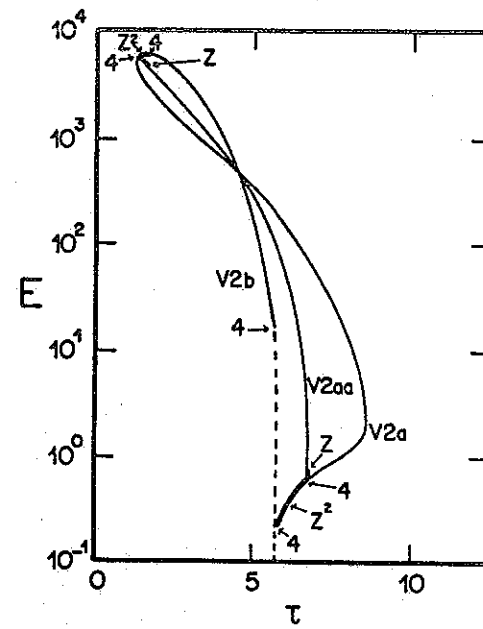


FIGURE 6

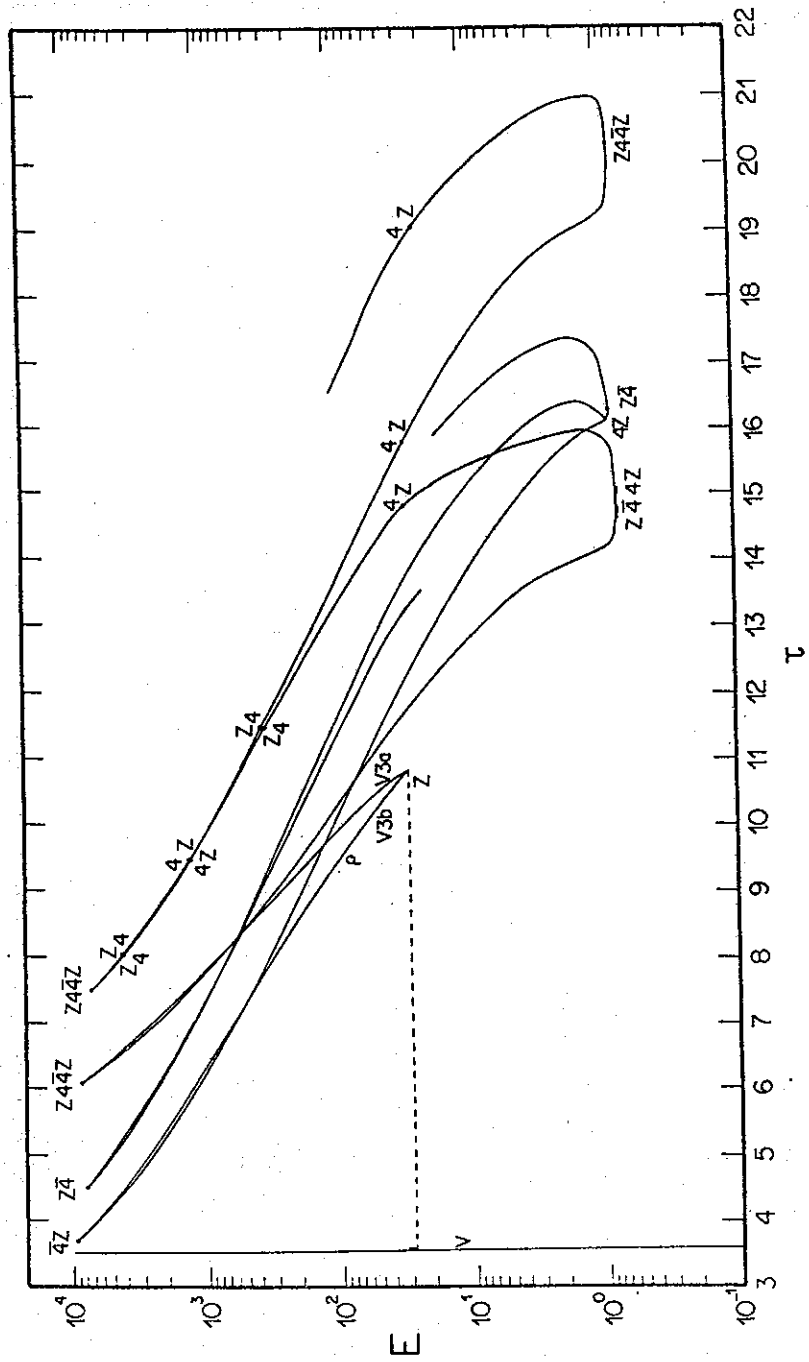


FIGURE 7

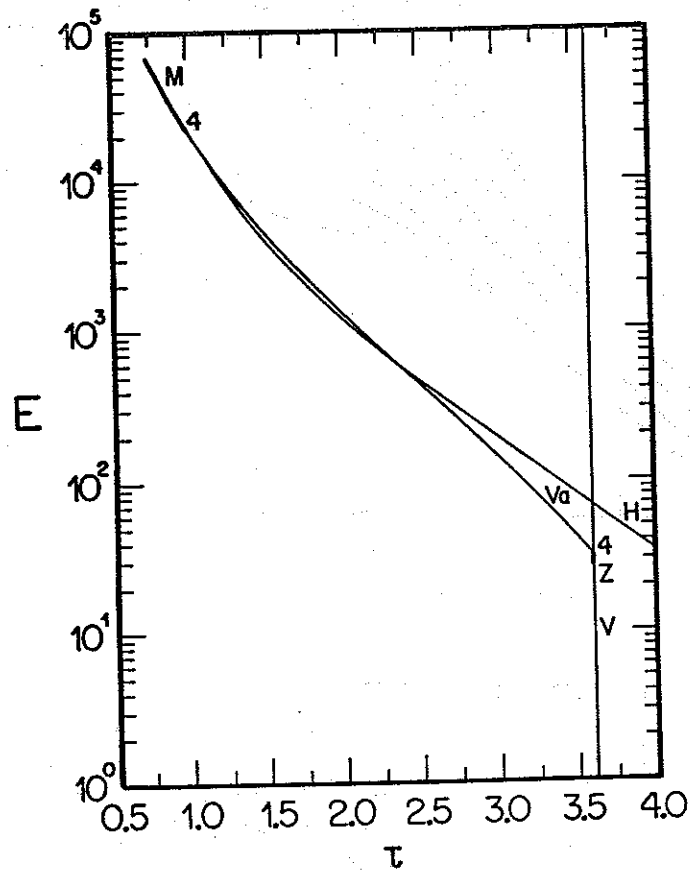


FIGURE 8

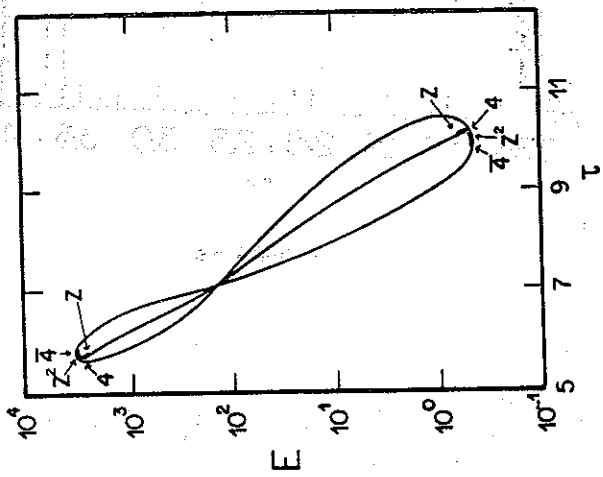
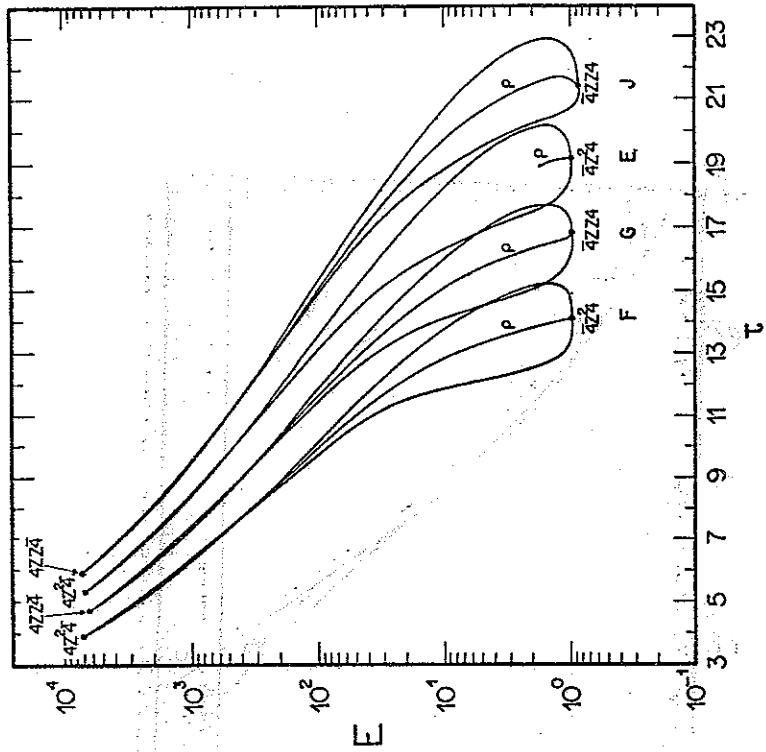


FIGURE 9

FIGURE 10

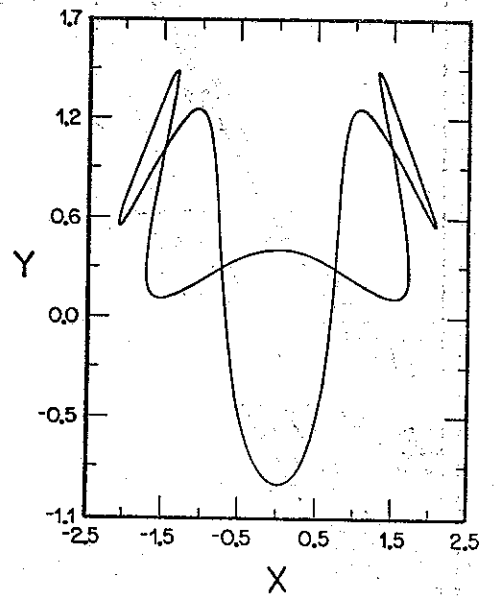
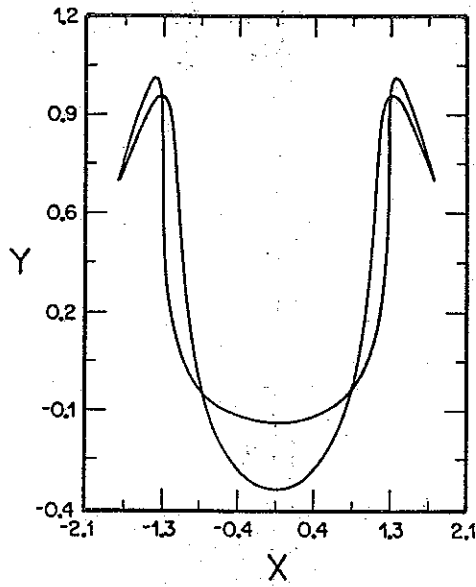
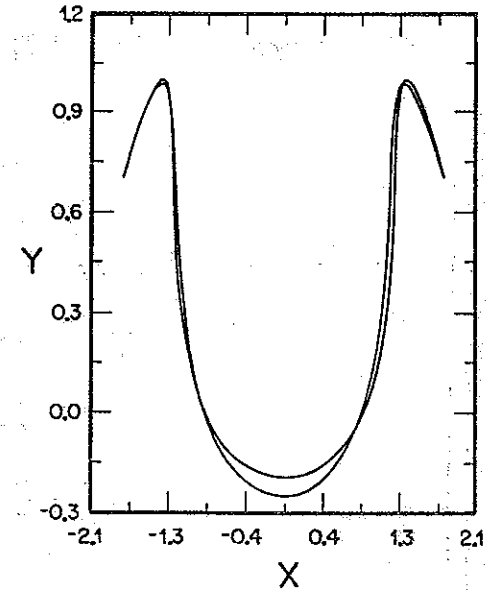
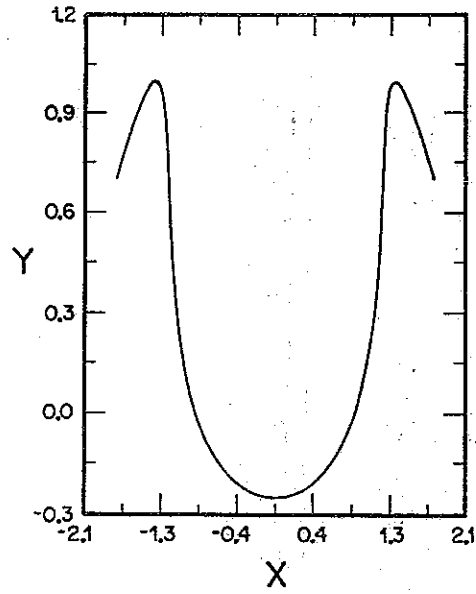


FIGURE 11

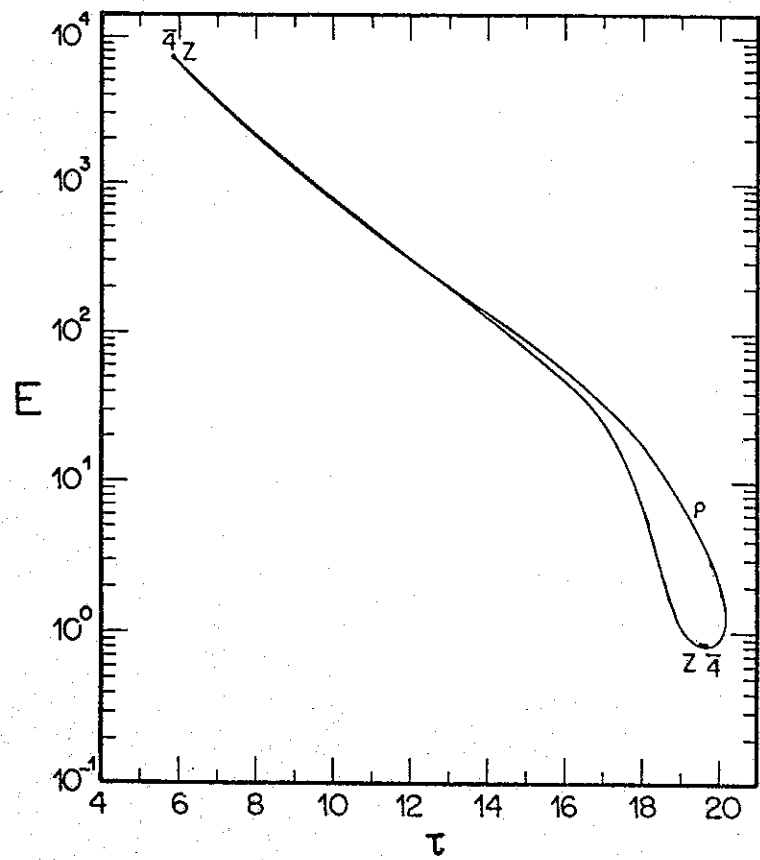


FIGURE 12

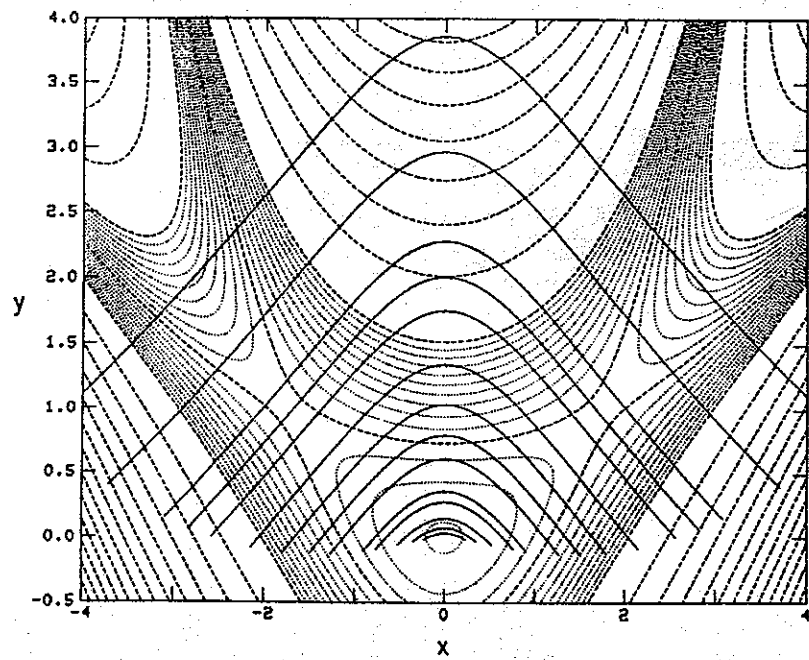


FIGURE 13

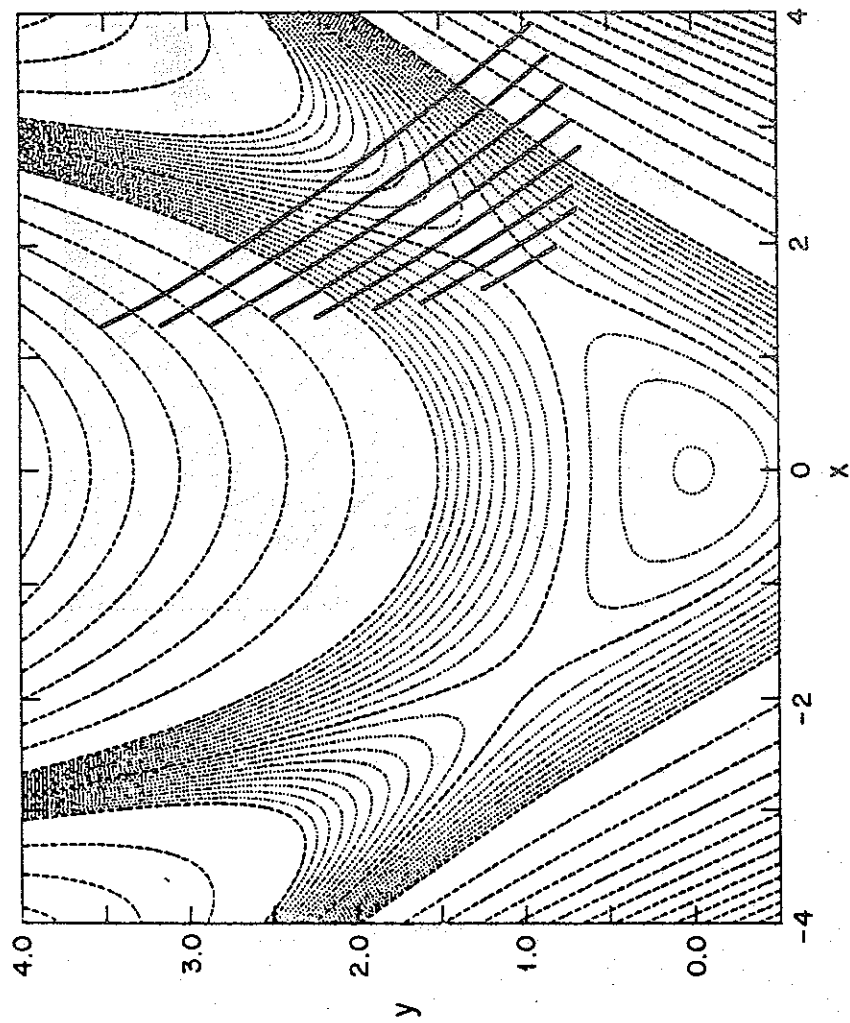


FIGURE 14

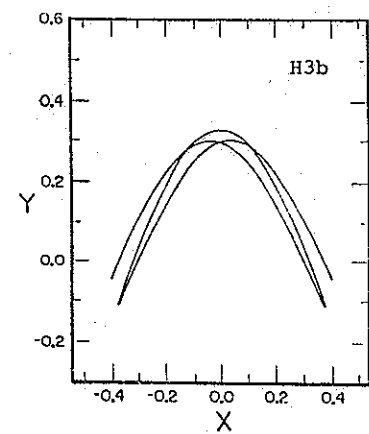
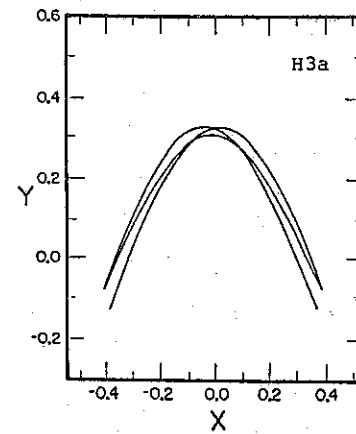
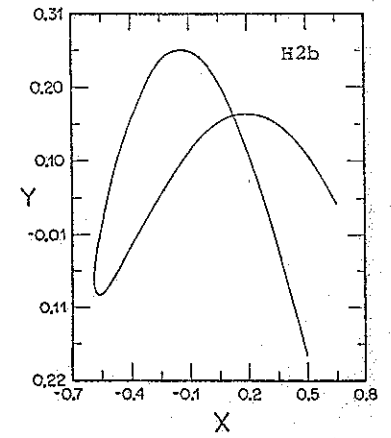
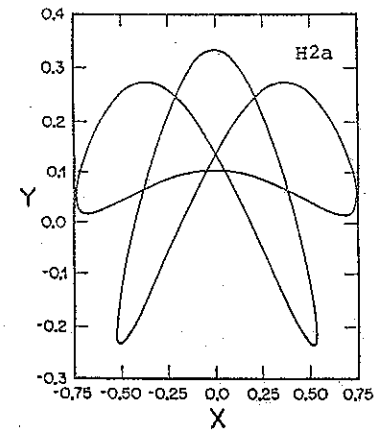
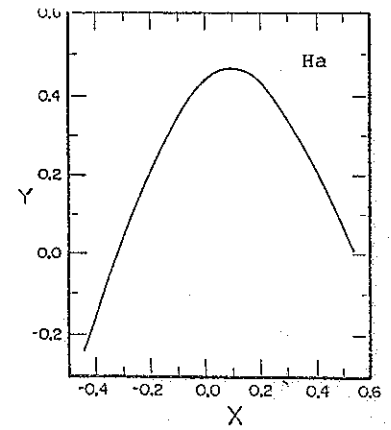
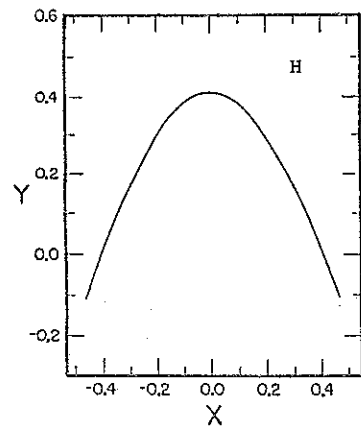


FIGURE 15

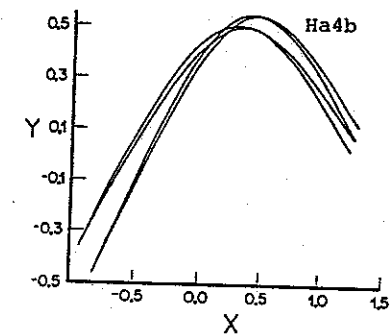
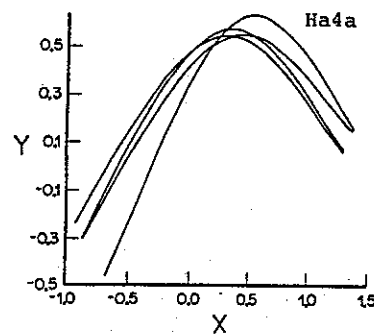
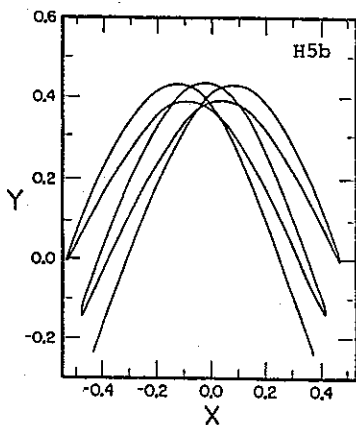
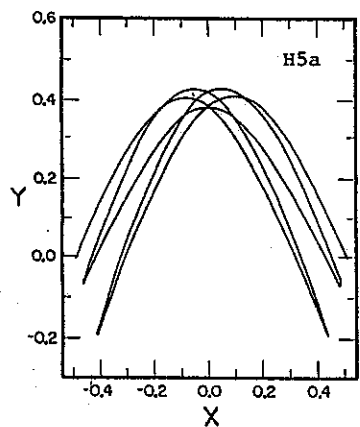
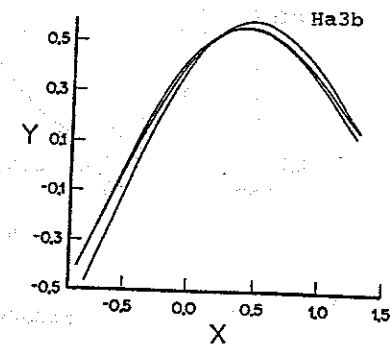
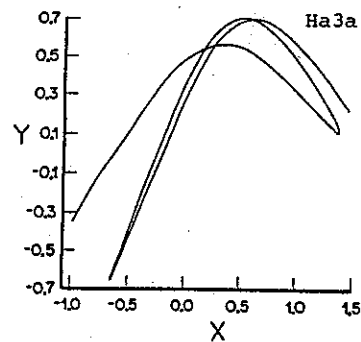
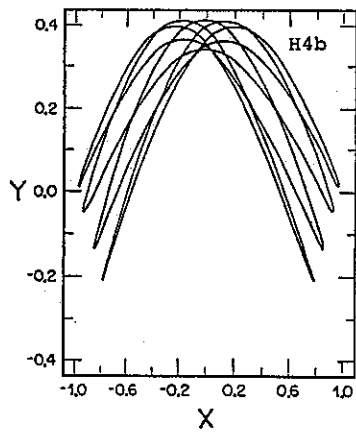
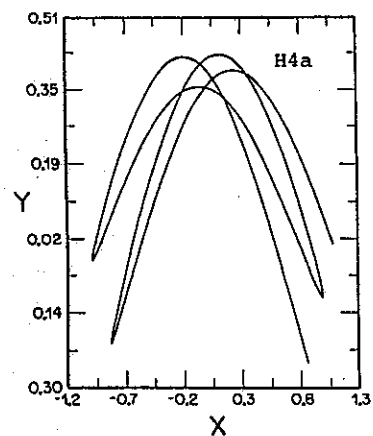
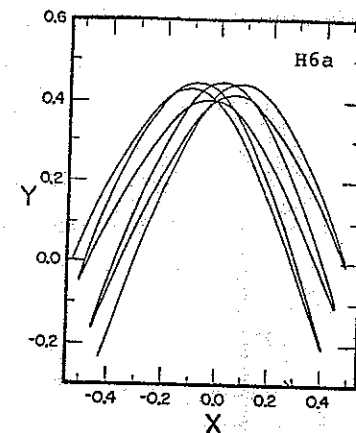
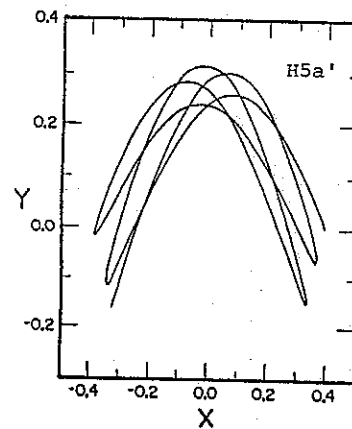
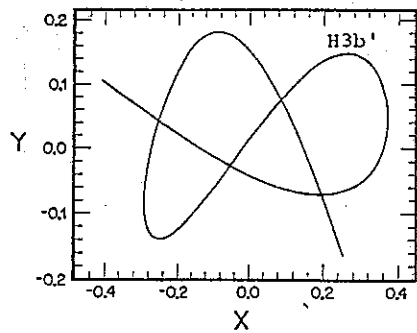
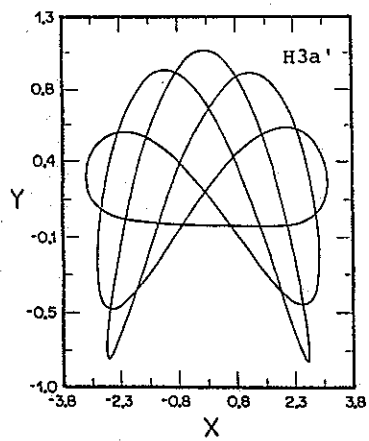


FIGURE 15 (cont.)

FIGURE 15 (cont.)

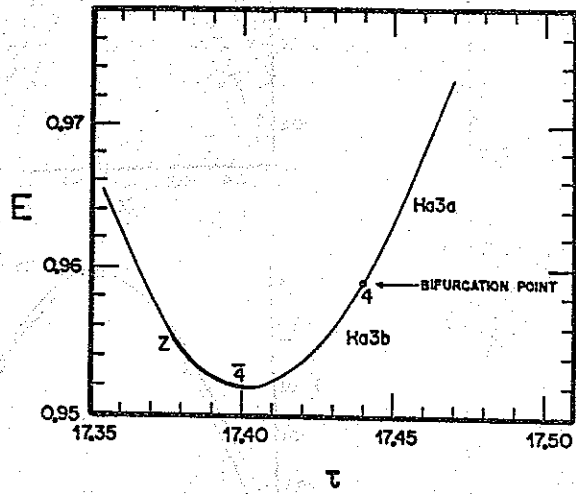


FIGURE 16

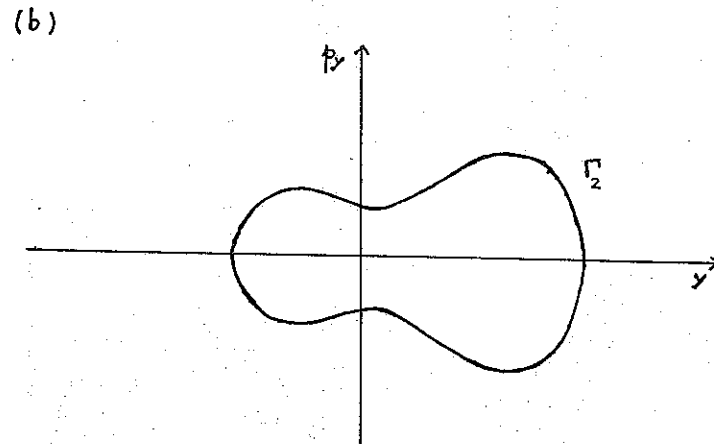
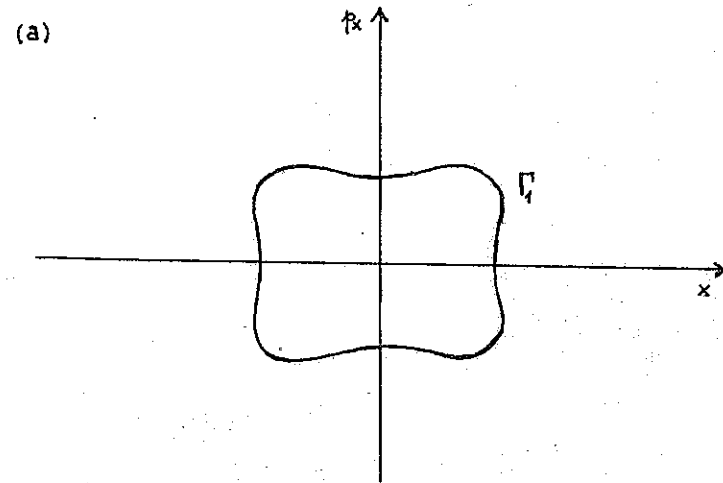


FIGURE 17

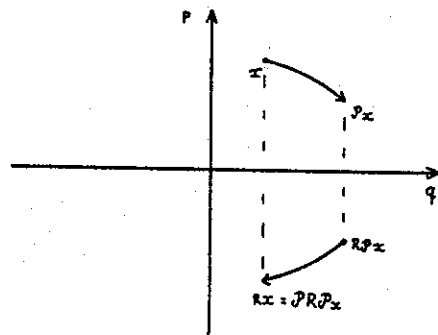


FIGURE 18